EXPRESSION ANALYSIS OF FORKED-LIKE FAMILY GENES DURING DEVELOPMENT AND IN RESPONSE TO NACL, ABA, AND AUXIN

KURTIS CLARKE
Bachelor of Science, University of Lethbridge, 2015

A Thesis
Submitted to the School of Graduate Studies
of the University of Lethbridge
In Partial Fulfilment of the
Requirements for the Degree

MASTER OF SCIENCE

Biological Sciences
University of Lethbridge
LETHBRIDGE, ALBERTA, CANADA

EXPRESSION ANALYSIS OF FORKED-LIKE FAMILY GENES DURING DEVELOPMENT AND IN RESPONSE TO NACL, ABA, AND AUXIN

KURTIS CLARKE

Date of Defence: April 30, 2018

Dr. E. Schultz Supervisor	Associate Professor	Ph.D.
Dr. I. Kovalchuk Thesis Examination Committee Member	Professor	Ph.D.
Dr. A. Russell Thesis Examination Committee Member	Associate Professor	Ph.D.
Dr. B. Selinger Chair, Thesis Examination Committee	Professor	Ph.D

Abstract

Auxin based developmental processes rely on PINFORMED (PIN) proteins for the polarized export of auxin. The protein FORKED1 (FKD1) influences PIN1 polarity in provascular cells and the subsequent formation of closed loops in leaf venation. Mutations to *FKD1* result in an open leaf vein pattern. *FKD1* is a member of the 9-member *FORKED-LIKE (FL)* gene family. While single mutants of *fl1*, *fl2*, and *fl3* result in no visible phenotype, a quadruple mutant of *fkd1/fl1-2/ fl2/fl3* has severely disconnected veins and reduced root elongation. This study was designed to observe the expression patterns of *FL*-gene family members by production of promoter-reporter constructs and the modifications of their expression by hormones or abiotic stresses. I found that members of this gene family are regulated by auxin, supporting their role in vascular tissue development. Moreover, their response to abscisic acid may indicate that the family is regulated in response to abiotic stress.

Acknowledgements

I would like to thank my supervisor Dr. Elizabeth Schultz for all the wonderful help and feedback she has provided despite the numerous setbacks and problems during the course of this thesis.

Thank you to the members of Schultz lab – Saabi, Houlin, Neema, Shankar, and Ryan- for their time, help, and discussions.

I am extremely grateful to the members of Kovalchuk lab – Nina, Rommy, Rocio, Andre, Bo, Ping, and Slava- for all their help and expertise.

I am grateful to Dr. Hongwei Hou and his lab members – Gaojie, Jingjing, Shiqi, Dr. Wu, Liangdan, and Prajani - that helped make my stay in Wuhan so enjoyable.

A special thanks to Dr. Aki Matsuoka who helped me occasionally get out of lab and enjoy the many wonders of Lethbridge I had never bothered to see.

Thank you to my committee members for their help, guidance, and suggestions during the course of this thesis.

Financial Support – Thank you to the University of Lethbridge, MITACS, AITF, and NSERC for the support in completing my Master's thesis.

Table of Contents

List of Tables

List of Figures

List of Abbreviations

Gene and Protein Abbreviation Annotation

FKD1 - the wild type gene is capitalized and italicized
fkd1 – the mutant gene is lower case and italicized
FKD1 – the protein is capitalized and unitalicized

T**ransfer DNA and Construct Abbreviation Annotation**

pFKD1:GUS – a shuttle vector containing a T-DNA where"pFKD1" is the gene promoter; ":" indicates fusion; and "GUS" is the β-glucuronidase reporter gene to which the promoter is fused.
pFKD1:GUS – italicized font indicates the genotype of an Arabidopsis line in which the T-DNA from the above vector has been integrated into the genome

Abbreviations

2,4-D	2,4-Dichlorophenoxyacetic Acid
ABA	Abscisic Acid
ABF	ABRE-Binding Factors
ABI1	ABA INSENSITIVE1
ABRE	Abscisic Acid Response Element
ADP	Adenosine Diphosphate
AREB	ABRE-Binding Proteins
ARF	AUXIN RESPONSE FACTOR
ARF-GAP	ADENOSINE DIPHOSPHATE RIBOSYLATION FACTOR- GUANOSINE TRIPHOSPHATE HYDROLASE ACTIVATING PROTEIN
ARF-GEF	GUANINE-NUCLEOTIDE EXCHANGE FACTOR ON ADP-RIBOSYLATION FACTOR G-PROTEIN (ARF-GEF)
ARP	ASYMMETRIC LEAVES1, ROUGH SHEATH2, and PHANTASTICA
Aux/IAA	AUXIN/INDOLE-3-ACETIC ACID PROTEINS
AUX1	AUXIN TRANSPORTER PROTEIN1
AuxRE	Auxin Response Element
AXR1-3	AUXIN RESISTANT1-3
BEN1	BRASSINOSTEROID INSENSITIVE1-5 ENHANCED 1-1DOMINANT
BFA	Brefeldin-A
BIG3	BREFELDIN A-INHIBITED GUANINE NUCLEOTIDE EXCHANGE PROTEIN3
BIG5	BREFELDIN A-INHIBITED GUANINE NUCLEOTIDE EXCHANGE PROTEIN5
CCA	CIRCADIAN CLOCK ASSOCIATED
CDKs	CYCLIN DEPENDENT KINASES.
CUC2	CUP SHAPED COTYLEDONS2
CVL1	COTYLEDON VASCULAR PATTERN2-LIKE
CVP2	COTYLEDON VASCULAR PATTERN2
DMSO	Dimethyl Sulfoxide
DRE	Dehydration Response Element
DREB	DEHYDRATION RESPONSE ELEMENT BINDING
DUF	Domain of Unknown Function
EE	Evening Element
EIN3	ETHYLENE INSENSITIVE 3

ERF1	ETHYLENE RESPONSE FACTOR 1
ETT	ETTIN
FKD1	FORKED1
FL	FORKED-LIKE
GNL	GNOME LIKE-1
GTPase	GUANOSINE TRIPHOSPHATE HYDROLASE
GUS	β-GLUCURONIDASE
HD-ZIPIII	CLASS III HOMEODOMAIN LEUCINE ZIPPER TRANSCRIPTION FACTORS
IAA	Indole-3-Acetic Acid
IAA-	De-Protonated Indole 3-Acetic Acid
IAAH	Protonated Indole-3-Acetic Acid
IND	INDEHISCENT
IPA	Indole-3-Pyruvic Acid
KAN	KANADI
LB	Lysogeny Broth Medium
LBamp100	Lysogeny Broth Medium Ampicillin 100 ug/mL
LBKan50	Lysogeny Broth Medium Kanamycin 50 ug/mL
MAPK	MITOGEN ACTIVATED PROTEIN KINASE
MIN7	HopM INTERACTOR7
MIR	Micro-RNA
MKK3	MITOGEN ACTIVATED PROTEIN KINASE KINASE3
NID	Non-ionic Detergent.
OD	Optical density
OSCA1	REDUCED HYPEROSMOLALITY-INDUCED (CA^{2+}) INCREASE 1
pFKD1:GUS	FORKED1 promoter:GUS reporter construct
pFKD1-A3:GUS	FORKED1 promoter:GUS reporter construct with the substitutions -1410T>G -844T>G -482T>G
pFKD1-ABRE:GUS	FORKED1 promoter:GUS reporter construct with the substitutions -1222T>
pFKD1-DRAB:GUS	FORKED1 promoter:GUS reporter construct with the substitutions -1222T>A-1208A>T
pFKD1-DRE:GUS	FORKED1 promoter:GUS reporter construct with the substitutions -1208A>T
pFL1:GUS	FORKED-LIKE1 promoter:GUS reporter construct
pFL2:GUS	FORKED-LIKE2 promoter:GUS reporter construct
pFL3:GUS	FORKED1-LIKE3 promoter:GUS reporter construct
PH	Pleckstrin Homology Domain
PI(4)P	phosphatidylinositol-4 monophosphate
PID	PINOID
PIF	PHYTOCHROME INTERACTING FACTORS
PIN	PINFORMED
PL	Pleckstrin Homology-Like Domain
PLT	PLETHORA
PP2A	PROTEIN PHOSPHATASE 2A
PP2C	PROTEIN PHOSPHATASE 2C
PYL	PYRABACTIN-RESISTANT1-Like

PYR	PYRABACTIN-RESISTANT1
QC	Quiescent Center
RAM	Root Apical Meristem
RCAR	REGULATORY COMPONENTS OF ABA RECEPTORS
SAM	Shoot Apical Meristem
SAS	Shade Avoidance Syndrome
SCF^{TIR1}	ASSOCIATED PROTEIN 1/CULLIN/F-BOX; where the F-box protein is TRANSPORT INHIBITOR1
SCF	SCARFACE
SnRK	SUCROSE NON-FERMENTING1-RELATED PROTEIN KINASES
SOS	SALT OVERLY SENSITIVE
TAA	TRYPTOPHAN AMINO TRANSFERASE
TAE	Tris-Acetate-EDTA Buffer
TGN	*trans*-Golgi network
TIR1	TRANSPORT INHIBITOR 1
TSS	Transcriptional Start Site
VAN3	VASCULAR NETWORK DEFECTIVE3
YUC	YUCCA

1.0 Introduction

Plants are sessile organisms that must respond to their environment in order to survive, and they often do so by modifying their growth and development. The flexibility of plant growth is due to indeterminate meristematic tissues that allow plants to modify their morphology throughout their lives. The morphological changes that plants go through are regulated by canonical developmental pathways that are influenced by the external environment. These developmental pathways and their modifications are regulated, in part, by the phytohormone auxin. Auxin regulates a broad range of developmental growth processes by influencing cell fate, division, and elongation, through auxin synthesis and transport (Zhao, 2010; Habets and Offringa, 2014). Processes influenced by auxin include leaf emergence, leaf morphology, root elongation, and root branching. This thesis focuses on the understanding of the aforementioned developmental processes based on discoveries in the model organism *Arabidopsis thaliana* (Arabidopsis). These developmental processes controlled by auxin are modified by a variety of environmental factors. For example, leaf development is noticeably affected by changes in water availability (drought or saline soils; Clauw et al., 2016; Kazachkova et al., 2013) and through changes in light availability (Xie et al., 2017). The shade avoidance syndrome (SAS), a plant response that causes reduced leaf size and elongated petioles, is regulated by the interactions of auxin with light sensing proteins. In roots, changes in nutrient availability can result in increased (NaCl; Zolla et al., 2010, nitrogen; Lima et al., 2010) or decreased (drought; Deak and Malamy, 2005; Seo and Park, 2009) lateral root to primary root growth allocations. These changes in leaf and root development, though heavily reliant on auxin, involve other hormone pathways, such as abscisic acid (ABA), that interact with auxin signaling. ABA is an important phytohormone that acts as a regulator of response to abiotic stresses, such as drought and salinity (Zhang et al., 2006). In chapter I will discuss the various roles of auxin synthesis and transport in development, the roles of ABA in drought and salinity response, and finally the role of the *FORKED-LIKE* (*FL*) genes in plant development and how they may influence developmental processes.

1.1 Cell response to Auxin

1.1.1 Auxin Biosynthesis

The most well characterized pathway of auxin biosynthesis occurs through modifications to tryptophan. The synthesis of auxin from tryptophan is a two-step process. The first step involves *TRYPTOPHAN AMINO TRANSFERASE* (*TAA)* family genes (*TAA, TAA-RELATED1, and TAA-RELATED2*) which convert tryptophan into indole-3-pyruvic acid (IPA) by their aminotransferase activity (Stepanova et al., 2008). IPA can then be converted into indole-3-acetic acid (IAA) by YUCCA (YUC) proteins (Won et al., 2011). The *YUC* gene family is highly redundant, with the mutation of several family members being required to show a phenotype. However the Arabidopsis phenotype when multiple *YUC* genes are mutated phenocopies the *taa1* mutant phenotype, indicating that these genes are likely acting in the same pathway (Won et al., 2011; Zhao, 2012). Mutations in auxin synthesis genes result in pleiotropic phenotypes that include changes to leaf morphology, venation, and floral development (Cheng et al., 2006).

1.1.2 Auxin Transport

The amount of auxin in cells is not only regulated by the synthesis of auxin, but also by the localization of auxin within tissues due to auxin transport by the PINFORMED (PIN) auxin efflux proteins (Adamowski and Friml, 2015). Auxin efflux is particularly important for the directional transport of auxin. In many tissues, auxin is able to passively enter cells because the acidic apoplast (pH 5.5), results in protonated IAA (IAAH) that can freely diffuse into cells. When IAAH enters cells, it is deprotonated to IAA^- (Robert and Friml, 2009), and, for subsequent export out of cells, it relies on PIN proteins, which can be polarly localized in cells. The polar localization of PIN proteins is dependent on the plant endomembrane system and post-translational modifications to PIN proteins. Generally, PIN proteins are localized to the membrane that faces the adjacent cell with the highest auxin concentration. This phenomenon creates a

positive feedback loop of auxin canalization that produces high auxin flux in tissues (Lee et al., 2014). Auxin canalization requires flexible recycling of PIN proteins, as the direction of auxin maxima may change as the auxin gradients are being formed (Habets and Offringa, 2014). PIN proteins are prone to lateral diffusion in the plasma membrane and need to be recycled to maintain a polar distribution. The rapid recycling of PIN proteins occurs by clathrin mediated-endocytosis to the trans-Golgi network (TGN) and re-secretion back to the plasma membrane allowing PIN to rapidly change membrane localization (Kleine-Vehn et al., 2011; Langowski et al., 2016).

There are at least two secretory pathways from the TGN involved in PIN secretion. The first, and best characterized, is the secretion to the basal plasma membrane via a pathway involving the GUANINE-NUCLEOTIDE EXCHANGE FACTOR ON ADENOSINE DIPHOSPHATE (ADP)-RIBOSYLATION FACTOR G-PROTEIN (ARF-GEF) GNOM and the related GNOM LIKE-1 (GNL1). GNOM/GNL1 have been shown to be required for the basal localization of PIN proteins through an early secretory pathway by mutant (Geldner et al., 2003) and pharmacological studies (Doyle et al., 2015). The reduction of basal polarity through disrupted GNOM secretion has multiple effects, including reductions in root length and agravitropism (Rahman et al., 2010). This basal pathway of PIN localization targets non-phosphorylated PIN to the plasma membrane. The phosphorylation status of PIN is regulated by PROTEIN PHOSPHATASE 2A (PP2A), which acts antagonistically to the PIN protein kinase PINOID (PID; Michniewicz et al., 2007). The phosphorylation of PIN by PID acts as the initial signal for the endomembrane system to re-localize phosphorylated-PIN to the apical membrane (Benjamins et al., 2001; Sukumar et al., 2009). Apical membrane localization of PIN occurs via a GNOM independent pathway, since disruptions of GNOM by pharmacological effects (Brefeldin-A; BFA and Endosin8) only result in basal polarity defects, not apical (Doyle et al., 2015). This non-GNOM apical pathway is less completely understood than the basal pathway, however, some of the proteins involved have been characterized. The apical localization of PIN is reduced in both

root and shoot tissue by mutations to *PID* (Zhang et al., 2010) and in developing leaf veins by mutation to *FORKED1* (*FKD1*; Hou et al., 2010). FKD1 is proposed to act in a BFA insensitive secretory pathway, and may be acting with a BFA insensitive ARF-GEF such as BRASSINOSTEROID INSENSITIVE1-5 ENHANCED 1-1DOMINANT/HopM INTERACTOR7/BREFELDIN A-INHIBITED GUANINE NUCLEOTIDE EXCHANGE PROTEIN5 (BEN1/MIN7/BIG5) or BIG3 to influence apical PIN localization (Doyle et al., 2015; Richter et al., 2014; Prabhakaran Mariyamma et al., 2017). In summary, basal PIN localization is regulated by the ARF-GEF GNOM/GNL1, while the incompletely characterized apical pathway involves FKD1, and phosphorylated PIN that may involve an alternative ARF-GEF to regulate PIN localization.

1.1.3 Auxin Response

Auxin is able to regulate gene expression through its modifications to protein interactions, specifically transcription factors. The direct regulation of genes by auxin in Arabidopsis occurs when auxin binds to TRANSPORT INHIBITOR 1 (TIR1), an F-box protein that acts as part of an S-PHASE KINASE ASSOCIATED PROTEIN 1/CULLIN/F-BOX (SCF^{TIR1}) complex, which ubiquitinate~~s~~ Auxin/IAA (Aux/IAA) proteins and causes their degradation (Dharmasiri et al., 2005). Aux/IAA proteins act to inhibit the expression of auxin responsive genes when auxin is not present, by binding to AUXIN RESPONSE FACTOR (ARF) proteins bound to the auxin response element (AuxREs), a *cis*-regulatory element in gene promoters. By degrading the Aux/IAA proteins, the activating ARFs are then able to trigger auxin-responsive transcription (Woodward and Bartel, 2005). Of the 22 ARF proteins only a few are activating (ARF5-8, ARF19; Guilfoyle and Hagen, 2007). The inhibitory action of repressive ARFs may be due to competitive inhibition with activating ARF proteins or other protein interactions. An example of the effects of ARFs on other protein interactions is the repressive ARF3/ETTIN (ETT) and its

interaction with INDEHISCENT (IND). The ETT-IND interaction is able to repress *PID* expression at low auxin concentrations, while at higher auxin concentrations the ETT-IND complex is destabilized and *PID* expression is induced (Simonini et al., 2016). The different ARF proteins are expressed in a tissue specific manner, which also influences the regulation of the activating and repressive ARFs (Rademacher et al., 2011).

1.2 Role of Auxin in Leaf Development

Leaf primordium development is initiated by a local auxin maximum that is created by a combination of auxin synthesis via YUC proteins (Guenot et al., 2012) and transport by PIN1 (Vernoux et al., 2010). Within the epidermis of the shoot apical meristem (SAM), the membrane localization of PIN re-orients to areas of higher concentration. The directed auxin transport results in a few cells having high auxin concentrations that initiate the outgrowth of a leaf primordium. As the newly initiated primordium begins to form, some of the apical, sub-epidermal cells begin to internalize auxin, predicting where the leaf mid vein will begin to form (Reinhardt et al., 2003; Heisler et al., 2005; Bayer et al., 2009; Deb et al., 2015).

Concurrently with the initiation of the midvein in the primordium, the polarity of the abaxial and adaxial sides of the leaf is established. The SAM appears to influence the adaxial identity, since ablating the outermost layer (L1) of the SAM resulted in a high frequency of radialized leaves with only abaxial identity (Reinhardt et al., 2004). The adaxial influence of the SAM is likely due, in part, to transient auxin depletion from the adaxial side of the primordium to the SAM (Qi et al., 2014). The differentiation between abaxial and adaxial sides of leaves involves several hormones and proteins. Overexpression of ARP protein family members (from ASYMMETRIC LEAVES1, ROUGH SHEATH2, and PHANTASTICA*)* in Arabidopsis results in highly adaxialized leaves, suggesting that ARP proteins specify the adaxial identity, even though mutants of ARP genes fail to show changes in leaf polarity (Yamaguchi et al., 2012;

Iwakawa et al., 2007; Lin et al., 2003). The Class III homeodomain leucine zipper transcription factors (HD-ZIPIII) are another group of proteins important for the specification of adaxial polarity, which are negatively regulated by micro-RNA (MIRNA) 165 and 166 that are expressed in the abaxial leaf side (Merelo et al., 2016). The adaxial ARP and HD-ZIPIII proteins mutually antagonize the abaxial determining KANADI (KAN) proteins, creating a stable boundary between the abaxial and adaxial domains (Izhaki and Bowman, 2007). Furthermore, *kan1/kan2* mutants have defects in abaxial specification that result in production of ectopic outgrowths on the abaxial side of the leaf (Abley et al., 2016). Since loss of *CUP SHAPED COTYLEDONS2 (CUC2)* greatly reduces the number of ectopic outgrowths, the outgrowths are proposed to be regulated by CUC2 (Abley et al., 2016). CUC2 expression is normally localized to the leaf margin where it causes leaf serration formation through changes in auxin and PIN localization (detailed description below). CUC2 activity is likely regulating this ectopic lamina expansion through a similar mechanism.

After the specification of adaxial and abaxial fate, leaves expand to form a blade by lamina outgrowth, which is mediated, in part, by YABBY proteins and auxin. The mutation of multiple *YABBY* genes results in the loss of leaf polarity maintenance and reductions in leaf lamina expansion, causing narrow leaves (Sarojam et al., 2010). Auxin also plays critical roles in lamina outgrowth. The mutation of multiple *YUC* genes result in narrow leaf phenotypes, supporting their requirement in leaf lamina expansion (Wang et al., 2011b). The narrow leaves of *yuc* mutants could also be due to disrupted central-marginal polarity, however the mechanism controlling central-marginal polarity is currently not well understood (Yamaguchi et al., 2012).

Leaf serrations are a special form of lamina outgrowth that are initiated by changes in auxin transport. The development of leaf serrations requires CUC2 for the repolarization of PIN1 at the leaf margin to produce an auxin convergence point by canalization (Figure 1.1). This auxin convergence point produces an auxin maximum that represses *CUC2* expression while promoting

leaf outgrowth (Bilsborough et al., 2011). The canalization of auxin to a maximum in the margin depletes nearby cells of auxin, allowing *CUC2* to remain expressed, which, since CUC2 represses leaf growth, results in sinuses between the serrations (Bilsborough et al., 2011; Blein et al., 2008; Kawamura et al., 2010).

1.3 Leaf Venation

Leaf venation and its modifications play important roles in plant productivity by influencing photosynthesis and plant survival in response to environmental conditions. The typical hierarchal, reticulate pattern of angiosperm venation has been a major advantage in angiosperm productivity over other plants (Zwieniecki and Boyce, 2014; Feild et al., 2011; De Boer et al., 2012). The structure of angiosperm venation allows the plant to maximize productivity by rapidly restoring water used in photosynthesis as a substrate and lost during the uptake of carbon dioxide while stomata are open (Fiorin et al., 2016). Vein structure becomes particularly important for plants in semi-arid environments that need to maintain productivity while surviving periods of decreased water availability. To adapt to arid environments, angiosperms have evolved higher levels of major vein density (Sack and Scoffoni, 2013). The increase in major vein density may be due to preference for smaller, thicker, and longer-lived leaves in arid environments that are transiently exposed to water (Gorai et al., 2015). By having higher major vein density, plants transiently exposed to increased water availability can have temporarily high photosynthetic rates, and maintain efficient water transport to the thicker mesophyll tissues reducing desiccation (de Boer et al., 2016).

The development of leaf venation is theorized to occur via auxin canalization. In molecular terms, auxin canalization is regulated by PIN1 proteins, which are initially distributed symmetrically around the plasma membrane. In response to changes in auxin distribution, the PIN1 proteins begin an auto-regulatory positive feedback loop through a “with the flux”

mechanism (Adamowski and Friml, 2015). Polarization of PIN protein localization results in the canalization of auxin transport into a subset of cells; the resulting high auxin concentration causes cells to adopt a vascular fate (Sauer et al., 2006)**.** The initial development of the midvein occurs during onset of primordium outgrowth. At this stage, PIN1 is apically localized in epidermal cells of the leaf margin. The resulting upward flow of auxin converges at the primordium tip, producing an auxin maximum that specifies the leaf apex (Reinhardt et al., 2003). Auxin spills from the convergence point at the leaf apex into the sub-epidermal cells below (Figure 1.1). In these cells, PIN1 is expressed and localized to the basal membrane, such that auxin is gradually canalized into a single line of cells that will become the midvein and transport auxin back to the SAM (Figure 1.2; Bayer et al., 2009). The formation of secondary veins in Arabidopsis occurs in two stages, the first being the formation of the lower loop domain and the second the formation of the upper loop domain (Figure 1.1). The formation of the lower loop begins in the leaf margin where an auxin maximum occurs about midway between the leaf tip and base. The auxin maximum is established by changes in PIN localization from apical to basal in the distal cells of the margin (Scarpella et al., 2006; Wenzel et al., 2007). As in midvein formation, this local auxin maximum then redirects auxin into the lamina, causing PIN1 expression in a domain that predicts the lower loop domain (Figure 1.1). PIN1 expression and basal localization extends towards the midvein, forming a connection. Next, expression of PIN1 is initiated in the upper loop domain, which extends towards the distal midvein (Scarpella et al., 2006). The connection of each upper loop domain with the apical midvein and lower loop domain requires a single bi-polar cell with both apically and basally localized PIN1, producing a continuous secondary vein connected to the midvein at two points.

Screens for leaf venation phenotypes such as abnormalities in vein meeting have identified, by mutation, several genes important for Arabidopsis leaf vein development. For example, mutation to *UNHINGED* (*UNH*) causes expanded PIN1 expression in lateral margin

cells. UNH is a member of the Golgi associated retrograde protein complex and is required for vacuole function and PIN1 degradation (Pahari et al., 2014). As described above, leaf serration and secondary venation are both initiated from PIN1 convergence points at the leaf margin. In *unh-1* leaves, the lack of PIN1 degradation in the leaf margin results in fewer, larger, and more persistent convergence points, that are proposed to cause larger serrations and more widely spaced, non-meeting secondary veins. The non-meeting venation is proposed to be a consequence of increased flux through the secondary vein compared to the midvein. Several venation phenotypes result from mutation to genes proposed to act in the apical PIN secretory pathway, including, *FKD1*, *SCARFACE/VASCULAR NETWORK DEFECTIVE3* (*SFC/VAN3*), *COTYLEDON VASCULAR PATTERN2* (*CVP2*), and *CVP2-LIKE* (*CVL1*). SFC/VAN3 is an ADP RIBOSYLATION FACTOR-GUANOSINE TRIPHOSPHATE HYDROLASE (GTPase) ACTIVATING PROTEIN (ARF-GAP), which appears to regulate vesicle trafficking. The *sfc/van3* mutant leaves have a discontinuous venation pattern (Koizumi et al., 2005; Sieburth et al., 2006). The localization of SFC/VAN3 is reliant on its pleckstrin homology (PH) domain that interacts with phosphatidylinositol-4 monophosphate (PI(4)P). The generation of PI(4)P occurs by the inositol polyphosphate 5'-phosphatases CVL1 and CVP2. The *cvl1/cvp2* mutant shows a similar venation phenotype to *sfc/van3*, which is supported by the cytosolic expression of SFC/VAN3 in the *cvl1/cvp2* mutant (Naramoto et al., 2009). SFC/VAN3 interacts with another protein, FKD1, which, when non-functional, results in a vascular discontinuity phenotype and shows reductions in apical PIN1 localization (Hou et al., 2010). Furthermore, the *sfc/fkd1* mutant shows increased discontinuous leaf venation compared to the single mutants, indicating that the function of the two genes overlap with each other (Steynen and Schultz, 2003; Naramoto et al., 2009). If the SFC/VAN3 PH domain is mutated, the FKD1 PH-LIKE (PL) domain is sufficient for the localization of SFC/VAN3, further supporting the interaction of these two proteins (Naramoto et al., 2009), and the requirement for PI(4)P in FKD1 localization (Prabhakaran Mariyamma et al., 2017). Both SFC and FKD1 localize to the TGN and to vesicles defined by

RABA-GTPases, which supports the hypothesis that FKD1 and SFC act in secretory processes (Prabhakaran Mariyamma et al., 2017) .

1.4 Root development

Similar to its role in leaf development, auxin plays several critical roles in Arabidopsis root development including controlling primary root length, gravitropic response, and the number of lateral roots. During embryogenesis, auxin, transported by PIN proteins, establishes the apical basal polarity in the hypophysis (Friml et al., 2003). The hypophysis provides the founder cells for the root quiescent center (QC; a group of less mitotically active cells) and the columella stem cells from which all root tissues are derived (Scheres et al., 1994; Petricka et al., 2012). The QC generates the surrounding initial cells, which then provide cells for the growing root tip including the vascular, endodermal, cortex, pericycle and epidermal cells (Petricka et al., 2012).

The root can be broadly divided into three apical-distal developmental zones, the meristematic zone, the elongation zone, and the differentiation zone (Figure 1.3). The meristematic zone is associated with cell divisions, and includes the QC, the initials and young cells near the root tip. Distal to the meristematic zone is the elongation zone that is distinguished by changes in cell length due to anisotropic growth from vacuole elongation (Cosgrove, 1993). Finally, the differentiation/maturation zone is distinguished by cell fate acquisition, visualized by the formation of root hairs and protoxylem vessels (Cajero Sánchez et al., 2017; Kondo et al., 2014).

Auxin is able to regulate root development by affecting cell differentiation via *PLETHORA* (*PLT*) genes, and cell division via the cyclin dependent kinases (*CDKs*). Auxin is initially transported from the shoot to the meristematic zone of the root apical meristem (RAM) by PIN proteins in the stele tissues. After auxin has been transported to the RAM from the shoot,

it is then laterally redistributed at the columella, and transported shootward through the root epidermis creating a “reverse fountain effect”, where it regulates root epidermal elongation. The regulation of cell division by auxin occurs through the upregulation of *CDKs* (Ferreira et al., 1994; Doerner et al., 1996) and the down-regulating *CDK* inhibitors (Sanz et al., 2011). The addition of exogenous 1-Napthaleneacetic acid (a synthetic auxin), results in increased cell proliferation supporting the role of auxin in cell proliferation. The *PIN* genes are also critical for normal RAM functioning, with all *pin* mutants affecting cell proliferation (Blilou et al., 2005). High levels of auxin promote cell proliferation in roots (Perrot-Rechenmann, 2010), in part due to the positive regulation of *CDK* and *CDK* related genes by auxin (Vanneste et al., 2005). The transition to the elongation zone is specified by an auxin minimum (Di Mambro et al., 2017) and a gradient of PLT family members influenced by auxin levels (Mähönen et al., 2014). The establishment of the apical-distal root zones is based on the PLT proteins, which act to separate the distinct root zones by inhibiting cell differentiation. *PLT* expression is focused in the QC, from which the gene products (mRNA or protein) diffuse into neighbouring cells to create a gradient of PLT proteins that specifies the unique root zones. *PLTs* require ARFs for their expression, however *PLTs* respond slowly to auxin likely through indirect activation (Mähönen et al., 2014). Interestingly, the inhibition of root elongation by ethylene was shown to increase auxin synthesis and the transport of auxin towards the shoot in the epidermis (Ruzicka et al., 2007; Swarup et al., 2007).

The distribution of auxin via the reverse fountain regulates not only root elongation in the primary root but also plays important roles in the development of lateral roots. The increased surface area provided by lateral roots allows plants to absorb additional water and nutrients from the soil. Lateral roots initiate in a periodic right-left alternating pattern based on the oscillatory expression of genes that regulate the specification of lateral root primordia cells (Moreno-Risueno et al., 2010). The exact signal specifying lateral primordia cells is not known, but some candidates

in Arabidopsis include ARF7 and LATERAL ORGAN BOUNDARIES DOMAIN 16 (Okushima et al., 2005; Moreno-Risueno et al., 2010). What is clear is that auxin signalling has several roles in the initiation and emergence of lateral root primordia. When the lateral root founder cells have been specified, an auxin maxima is created by auxin biosynthesis and transport to specify the fate of a single cell file to become a lateral root (Swarup et al., 2008; Péret et al., 2013). When auxin influx *AUXIN TRANSPORTER PROTEIN1* (*AUX1*) or efflux carrier genes (*PIN2/PIN3/PIN7*) are mutated, the branching pattern of lateral roots is transformed with closely grouped, and sometimes even fused lateral root primordia occur (Laskowski et al., 2008; Du and Scheres, 2018).This would indicate that, as in the developmental processes controlled by auxin discussed previously, PIN mediated auxin canalization is important to prevent ectopic lateral root formation in areas of the pericycle competent for lateral root formation.

1.5 Regulation of plant gene expression by ABA

Plant development is also affected by the phytohormone ABA that regulates gene expression in several circumstances, in particular, those relating to abiotic stress. In the canonical ABA response pathway of Arabidopsis, ABA binds to PYRABACTIN-RESISTANT1/PYR1-LIKE/REGULATORY COMPONENTS OF ABA RECEPTORS (PYR/PYL/RCAR) receptors, causing a conformational change in the receptor so they can bind to ABA INSENSITIVE1 (ABI1) a PROTEIN PHOSPHATASE 2C (PP2C). The interaction of PYR/PYL/RCAR with ABI1 competitively inhibits the interaction of ABI1 with SUCROSE NON-FERMENTING1-RELATED PROTEIN KINASES (SnRK2.2/3/6; de Zelicourt et al., 2016). The SnRK2 proteins, once free from ABI1, can then phosphorylate downstream transcription factors to modify the activity of other ABA response proteins (de Zelicourt et al., 2016). The PYR -| PP2C -| SnRK2 signal cascade triggers broad effects by signalling MITOGEN ACTIVATED PROTEIN KINASE (MAPK) cascades which have their own phosphorylation targets. Specifically, the MAPK3/17/18

pathway is important for ABA-dependent responses, and may be triggered by ABA responsive SnRK2.2/3/6 either directly or indirectly (de Zelicourt et al., 2016). The role of this MAPK KINASE3 (MKK3) related MAPK module in long term drought response is shown by studies where MAPK impaired plants were unable to respond appropriately to drought. The SnRKs and MAPKs regulate ABA responses by activating proteins such as the ABRE-binding proteins/ABRE-binding factors (AREBs/ABF) transcription factors through phosphorylation.

The phosphorylation of AREB/ABF (ABF 1-4) by drought responsive SnRK2s (SnRK2.2/3/6), allows these TFs to influence gene expression by targeting specific *cis*-regulatory elements in gene promoters such as the ABA-response element (ABRE; Yoshida et al., 2015). AREB/ABF factors are context specific and may act as both transcriptional activators and repressors (Finkelstein, 2013). The ABRE element (PyACGTGG/TC) was previously identified as a conserved *cis*-regulatory element in ABA response (Guiltinan et al., 1990; Mundy et al., 1990; Busk and Pagès, 1998; Choi et al., 2000; Shinozaki and Yamaguchi-Shinozaki, 2000). Noticeable changes in gene transcription were found to require at least two ABRE elements or one ABRE element combined with an additional coupling element (Narusaka et al., 2003). Potential coupling elements include MYB, evening elements (EE; Mikkelsen and Thomashow, 2009) and drought response elements (DRE), the latter interaction was identified in the study of the *RD29A* promoter through deletion and mutagenesis (Narusaka et al., 2003).

1.6 Drought and Salinity

1.6.1 Plant Drought and Salinity Sensing

The exact mechanisms for sensing abiotic stresses, like hyper-saline and drought conditions, are not well understood. Both drought and salt responses involve ABA dependent and independent response pathways (Vishwakarma et al., 2017). Thus, they share some common elements, but are not exclusively overlapping, indicating unique but poorly characterized sensing mechanisms.

Drought and salt stress also have overlapping molecular responses due to their hyperosmotic effects on cells, which alter cell turgor pressure (Zhu, 2016). A clear pathway of sensing osmotic stress has not been elucidated, however, potential sensory response mechanisms to hyperosmotic stress include organellular sensing mechanisms (Chloroplasts; Chan et al., 2016, or mitochondria; Vanderauwera et al., 2012) and calcium signalling. Calcium signalling appears to be particularly likely based on the discovery of REDUCED HYPEROSMOLALITY-INDUCED (CA^{2+})INCREASE 1 (OSCA1), which is a plasma membrane hyperosmolarity-gated calcium-permeable channel (Yuan et al., 2014). Arabidopsis *osca1* mutants do not show drought or salt stress phenotypes, perhaps because they cannot respond to the calcium influx that signals osmotic stress (Huang et al., 2017). The influx of calcium influences calcium interacting proteins, altering a variety of responses including nuclear signalling (Guan et al., 2013). As such, a plausible explanation for the *osca1* phenotype is that lack of an osmosensing Ca^{2+} channel would eliminate the Ca^{2+} response pathway and prevent plants from responding correctly to drought or osmotic stress.

Salt stress not only causes hyperosmolarity, but also causes ion toxicity that plants need to respond to. Again, no direct mechanisms of salt stress have been found, though the salt response is known to occur through the SALT OVERLY SENSITIVE (SOS) pathway (Ji et al., 2013). The SOS pathway involves three members, SOS1/2/3. In response to salt stress, SOS3 (an EF-hand calcium binding protein) senses a change in cytosolic calcium triggered by salt stress, and interacts with the ser/thr protein kinase SOS2 to phosphorylate SOS1 (Du et al., 2011). The activation of SOS1 (a plasma membrane Na^+/H^+ antiporter) by phosphorylation, allows the export of NaCl to the soil and xylem. SOS2 appears to regulate most of the changes in gene expression through its phosphorylation of proteins that alter gene expression such as ABI2 (Ohta et al., 2003) and ETHYLENE INSENSITIVE 3 (EIN3; Quan et al., 2017). The ABI2 interaction is important for influencing seed germination (Trupkin et al., 2017), while the phosphorylation and

stabilization of EIN3 deters reactive oxygen species accumulation in salt stressed roots (Peng et al., 2014).

1.6.2 Drought, Salinity, and Gene Expression

Drought responses are linked to the DRE-BINDING (DREB) 1A-C, DREB2A, and DREB2B proteins (Lata and Prasad, 2011). The DREB1A-C proteins are also known as cold binding factors due to their more important role in cold responses (Novillo et al., 2004). In contrast, DREB2A and DREB2B proteins have their most important roles in drought, salt, and osmotic stresses (Liu et al., 1998; Nakashima et al., 2000; Sakuma et al., 2002). These drought responses are triggered by a separate set of cis-regulatory elements including the core DRE element (A/GCCGAC; Kasuga et al., 1999; Masson et al., 2002). The DREB2 proteins, which bind to DRE elements, can couple with ABRE elements to provide a drought specific upregulation of genes (Narusaka et al., 2003). ABA itself is involved in the upregulation of DREB2A (Kim et al., 2011), though other mechanisms such as phosphorylation and activation of DREB2A may play important roles in its effectiveness (Morimoto et al., 2013). ABA and DREB2A concentrations are highest within the first 24 hours of drought treatment. During these first 24 hours, ABA and DREB2A proteins interact to regulate drought responsive genes through cis regulatory elements. The ACGTGTC/A ABRE is most common in early upregulated genes, while the AAACGTG ABRE motif is more common in late expressing drought genes. Furthermore, presence of DRE was found to increase gene expression in early drought (within 1 day), but not at later time periods (Harb et al., 2010). This results in time dependent changes either via short-term responses, such as modifications to root growth, or if the stress is severe and prolonged, plants may try escape the drought stress by going to seed. The variance in the gene ontology expression profiles of early and late time points during prolonged drought stress can likely explain the regulation of these different responses (Su et al., 2013; Kazan and Lyons, 2016).

1.7 Plant Developmental Changes in Response to Environment

1.7.1 Response of Leaf and Root to drought

In plants that are able to acclimate to drought, roots and leaves undergo multiple morphological changes to increase resistance to drought. Root biomass increases, and many plants, such as Arabidopsis, reduce lateral root formation while maintaining primary root growth. The change in root growth strategy allows plants to burrow deeper into the soil to reach a lowered water table (Basu et al., 2016; Koevoets et al., 2016). Leaves also undergo several morphological changes. Some common acclimations include reduced leaf size, increased leaf thickness, increased major vein density, and the formation of a waxy cuticle (Sack and Scoffoni, 2013; Scoffoni et al., 2013; Bi et al., 2017). Reduced size and increased thickness of leaves decreases the surface area of a leaf available for both transpiration and photosynthesis. In hot and dry environments, smaller leaves absorb less heat and are more quickly cooled, reducing transpiration (Sack and Scoffoni, 2013). The increased thickness of a plant's waxy cuticle reduces transpiration through non-stomatal pathways (i.e. the epidermis) reducing overall water loss at the cost of wax formation (Kosma et al., 2009; Guo et al., 2013). Older plant leaves, in response to ABA, can preferentially begin to senesce, reducing plant transpiration and developing greater osmotic potential gradients that may increase the water transport to younger leaves (Zhao et al., 2016). Plants that undergo prolonged drought may also induce a transition of the vegetative meristem to the reproductive, reducing plant flowering time to rapidly produce seed under stressful conditions (Kazan and Lyons, 2016).

1.7.2 ABA, a Signal for Abiotic Stress

ABA acts as the initial signal to trigger plant acclimations to several abiotic stresses including drought and salinity. The initial sensing of drought can occur in leaves or roots to signal ABA synthesis in specific tissues. Roots signal the synthesis of shoot ABA via an unknown signalling

pathway, while shoot-root ABA transport can directly modify root ABA levels (McAdam et al., 2016; Manzi et al., 2015; Waadt et al., 2014; Jones et al., 2014). After the propagation of the ABA signal, plants begin to induce changes in physiological responses and gene expression that start plant acclimation. Initially, ABA signals the rapid closure of stomata that reduces plant transpiration and water loss. During prolonged drought, plants begin to accumulate osmolites such as proline and raffinose to increase the osmotic potential of plant cells to reduce water loss (Krasensky and Jonak, 2012). If drought continues, plants begin to alter their developmental programs in a tissue specific way to acclimate to the harsh conditions.

1.7.3 Hormone Interactions Influence Root Development during Stress

In order to influence root growth, ABA interacts with other hormones including auxin and ethylene. ABA has biphasic effects on Arabidopsis root development, promoting root growth at low concentrations by interactions with auxin, and inhibiting root growth at high concentrations by ethylene interactions (Li et al., 2017). Although ABA and ethylene response pathways often antagonize each other (Cheng et al., 2009), the two pathways work together in response to stress conditions. ETHYLENE RESPONSE FACTOR1 (ERF1) increases ABA expression, which in turn down-regulates ERF1 and the expression of ethylene synthesis genes (Cheng et al., 2013). The induction of ABA downregulates the response of many auxin related genes by upregulating the repressive ARF2, which has been shown in roots to repress *PIN* gene expression (Promchuea et al., 2017). ARF2 has been linked to a reduction in cell proliferation and expansion during leaf development, resulting in smaller leaves (Lim et al., 2010). Interestingly, since treatment with either ethylene inhibitors or auxin influx inhibitors significantly reduce ABA induced root shortening compared to ABA alone, the inhibition of root growth at high ABA levels seems to require both ethylene response and auxin influx pathways (Li et al., 2017). The stimulatory effects

of low ABA on root growth also involve changes in auxin transport, as the increased growth at low ABA is inhibited by the *pin2* mutant (Thole et al., 2014; Li et al., 2017).

1.7.4 Gravitropism

Plants alter auxin transport in response to changes in their environment, such as, when roots are moved so they are no longer oriented towards gravity. The re-orientation of roots towards gravity, known as gravitropism, is regulated by auxin, and allows plants to reach subterranean water and nutrients (Band et al., 2012). Root gravitropism is a three-step process involving perception of a change root position relative to gravity, signal transduction, and asymmetric growth (Singh et al., 2017). The initial sensing of a change in root gravity likely occurs through the sedimentation of starch filled amyloplasts, known as statoliths, in the root columella cells towards the cell membrane that faces gravity (Leitz et al., 2009). However, the columella cells where gravity is sensed, and the root epidermal cells that respond to changes in gravity are spatially separated. The transduction of root gravitropic signals is caused by the endocytosis of PIN3 and PIN7 from the lateral plasma membranes of the columella cells and their re-localization to the membrane that faces gravity. This change in PIN localization, and the resulting auxin export, results in auxin asymmetry on one side of the root tip. The change in auxin is then distributed up through epidermal cells by asymmetrically localized PIN2 and the AUX1 influx proteins (Rigas et al., 2013; Rahman et al., 2010). The asymmetric shootward localization of PIN2 is regulated in part by PID (Sukumar et al., 2009). The high levels of auxin on one side of the epidermis then reduce the elongation of the root epidermal cells facing gravity, causing the root to bend towards gravity as the cells on the other side of the root continue to elongate.

1.7.5 Shade Avoidance Syndrome

In natural ecosystems, plant often grow to escape shade in a process known as shade avoidance syndrome (SAS) that is regulated by changes in auxin synthesis and sensitivity. Auxin acts to coordinate SAS which causes increased petiole length and reduced leaf size. Plants sense shade by the ratio of far-red to red light. Since far-red light is reflected by neighbours, while red is absorbed, the ratio of the two gives an indication of shading. Changes in far-red to red light ratios are sensed by the *PHYTOCHROME INTERACTING FACTOR* (*PIF*) genes in Arabidopsis, which induce SAS. PIF7 (and partially redundant PIF4 and PIF5) upregulate *TAA1* and *YUC* (auxin biosynthesis genes), increasing auxin synthesis (Tao et al., 2008; Li et al., 2012; Procko et al., 2014). The importance of auxin synthesis to SAS responses is shown by the impaired SAS responses in both the *taa1* and the *yuc2/yuc5/yuc8/yuc9* quadruple mutant. Auxin transport has been shown to regulate SAS by the addition of N-1-naphthylphthalamic acid (NPA) to the petiole-blade junction, which severely inhibited petiole elongation in response to high far-red to red ratios (Kozuka et al., 2010). Consistent with the NPA result, *pin3-3* mutants also have impaired SAS responses (Tao et al., 2008). Interestingly, auxin concentrations have been reported to change in petioles during SAS but not in leaf blades. The change in leaf blade SAS responses occurs due to a change in auxin sensitivity, not concentration (de Wit et al., 2015). Thus, though auxin synthesis is modified by shade, auxin sensitivity and transport may play more important roles in shade avoidance responses.

1.8 The *FKD1* and the *FL* Gene Family

Further understanding the plant proteins involved in PIN localization, of which FKD1 and its homologues are potential candidates, will help to understand the aforementioned processes of plant development. *FKD1* was identified in Arabidopsis as part of a family of proteins known as the FORKED-LIKE (FL) family defined by their Domain of Unknown Function (DUF828;

Prabhakaran Mariyamma et al., 2018 in revision). All of the FL-protein family members, except for FL4, contain a PH or a PL domain, which has been shown in other proteins to interact with phosphoinositides, suggesting that all members may be localized via membrane phospholipids. The *FL* genes are divided into 3 groups based on sequence homology; group I *FL* genes include *FKD1*, *FL1*, *FL2*, and *FL3*. The group I *FL*-genes likely originated in the basal Angiosperm *Amborella trichopoda*, which has a single gene that is homologous to the group I *FL*-genes. Interestingly, reticulate venation emerged in *Amborella trichopoda*, suggesting that the evolution of group 1 *FL*-genes may have allowed the formation of distal vein junctions in leaves (Prabhakaran Mariyamma et al., 2018 in revision). Arabidopsis itself is a member of the dicotyledonous Brassicaceae family and discoveries in Arabidopsis will be particularly applicable to closely related crop species (canola, broccoli, cabbage, etc). Furthermore, multiple copies of FL genes seems to be ubiquitous in vascular plant genomes (Prabhakaran Mariyamma et al., 2018 in revision), suggesting that the gene family may have broad importance in the localization of PIN proteins and auxin transport.

Within Arabidopsis group I *FL*-genes, FKD1 is the most divergent protein which may explain its prominent single mutant phenotype, with distally non-meeting veins due to lack of PIN1 localization on the apical sides of cells (Steynen and Schultz, 2003; Hou et al., 2010). Similar to *fkd1*, the *fkd1/fl2/fl3* mutant shows reductions in the polarization of PIN1 compared to wild-type. It is possible that the *fkd1/fl2/fl3* mutant has more severe defects in PIN localization than the *fkd1* mutant as the data between two studies at similar developmental stages would suggest (Hou et al., 2010; Prabhakaran Mariyamma et al., 2018 in revision). The other group I *FL* family members do not show an obvious phenotype when single genes are mutated, potentially due to genetic redundancy (Prabhakaran Mariyamma et al., 2018 in revision). However, multiple mutation of the group I *FL* genes (*fkd1/fl2/fl3* and *fkd1/fl1-2/fl2/fl3*) results in more severe reductions in vein meeting, indicating that the *FL*-genes may have some overlapping functions in

leaf vein development, potentially in PIN localization. The *fkd1/fl1-2/fl2/fl3* and *fkd1/fl1-2* mutants also show novel phenotypes not seen in single mutants such as reductions in root elongation and gravitropic response (Yu, personal communication). This similar root phenotypes may indicate that FKD1 and FL1 are compensating for each other. The *fkd1/fl2/fl3* and *fkd1/fl1-2/fl2/fl3* mutants also show leaf epidermal cell polarity defects that result in leaf deformities such as buckling. The phenotype of the *fkd1/fl2/fl3* mutant supports the role of the *FL* gene family in cell polarity perhaps due to the reduction in the polar localization of PIN in several developmental stages. To better understand the expression of these genes and their role in plant development I opted to look at their expression in tissues and the factors that may be regulating expression.

1.9 Hypotheses

1. Based on the roles of FKD1 in auxin canalization and the enhancement of the *fkd1* phenotype by mutation to other *FL*-genes in the *fkd1/fl1-2/fl2/fl3* mutant, I hypothesize that the other group I *FL*-gene family members are expressed in developing tissues in a manner similar to FKD1 including expression in the leaf venation, leaf epidermis, and the root apical meristem.

2. Based on the role of auxin transport in plant development and environmental responses, I hypothesize that the expression of the *FL*-genes is modified by auxin, ABA, salinity, and osmotic stresses, and that the mutation of key elements in the *FKD1* promoter can alter these responses.

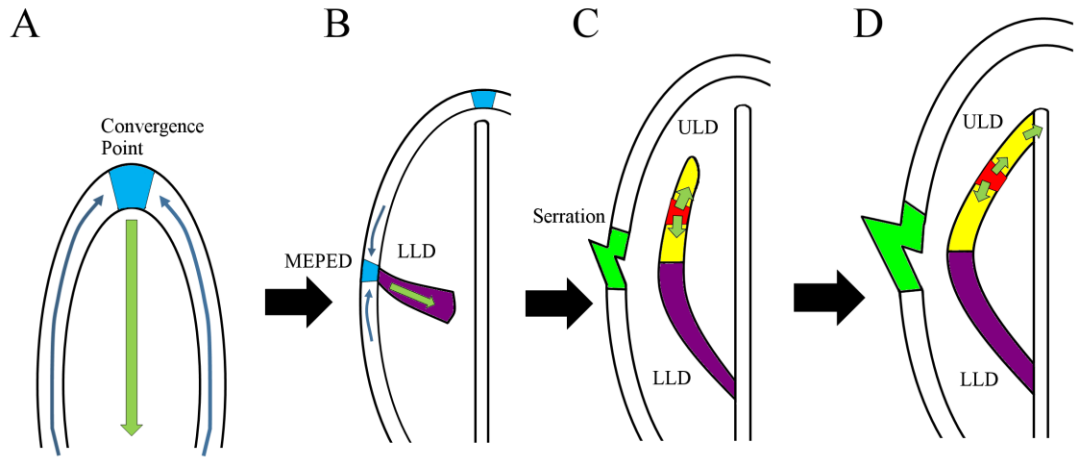

Figure 1.1: Development of a stereotypical Arabidopsis leaf. (A) Initially during primordium development, a convergence point of auxin is generated at the tip of the leaf by PIN directed auxin transport through the marginal epidermal cells (blue arrows). Auxin at the convergence point is then internalized, and induces PIN expression in presumptive midvein. The basal localization of PIN1 results in basal auxin transport (green arrow). (B) At later stages of development, additional marginal epidermal PIN expression domain (MEPEDs) generate auxin maxima from which auxin begins to be internalized by PIN proteins (green arrow). The lower loop domain (LLD, purple) of a secondary vein is initiated by this internalization of auxin. (C) Subsequently the upper loop domain (ULD; yellow) which includes a bipolar cell (red) that localizes PIN to opposite cell membrane faces (green arrows) begins to form. Additionally, the high auxin concentration at the MEPED may generate a leaf serration. (D) Eventually the upper loop domain connects with the midvein to form a secondary vein loop.

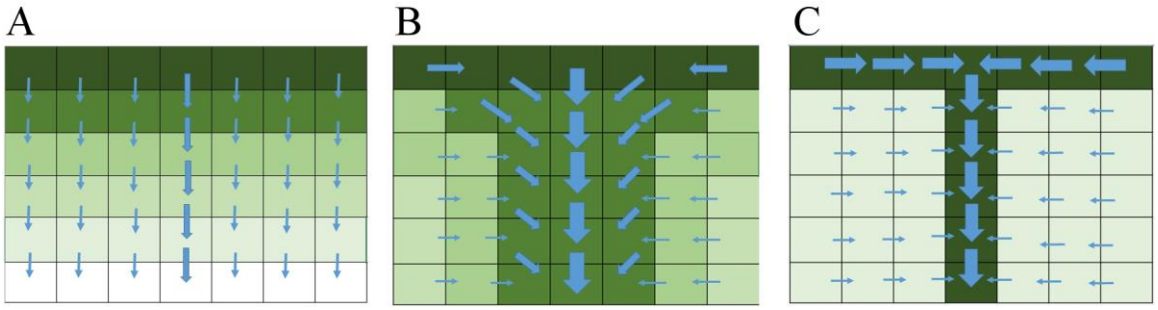

Figure 1.2: Diagram of auxin canalization. Intensity of green indicates level of cellular auxin, while blue arrows indicate the direction of PIN localization within a cell. (A) Initially cells export auxin to adjacent cells. (B) As a group of cells begins to export more auxin than other adjacent cells, auxin concentration and PIN proteins levels increase in this group of cell cells resulting in a group of cells with high auxin and PIN levels. (C) Eventually the group of cells is narrowed down to a single file of cells which are specialized to export auxin and will ultimately become the vascular tissue.

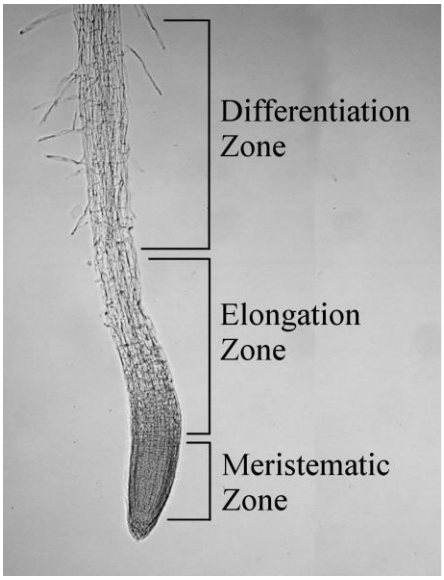

Figure 1.3: Developmental zones on a wild type Arabidopsis root. The meristematic zone occurs at the tip of the root where cells are actively dividing and before cells begin to elongate. The elongation zone is marked by an increase in cell length. Finally, in the differentiation zone, cells begin to acquire their cell fate, which is visible as the formation of root hairs on the epidermal cells.

2.0 Materials and Methods

2.1 Plasmid Extraction

Plasmid extractions were done using either a highspeed plasmid miniprep kit (Froggabio), or a QuickPure Plasmid Minikit (CWBIO) according to the manufacturer's protocol. A Non-Ionic Detergent (NID) miniprep was also used due to its low cost and high yields for plasmid detection and sequencing based on a published protocol (Lezin et al., 2011), except that 0.5 M NaCl was used in place of 0.75 M NH_4Cl.

2.2 Generating Electro-competent Cells

2.2.1 *Escherichia coli*

Electro-competent DH5-α *Escherichia coli* cells were prepared based on a published protocol (Untergasser, 2008; http://www.molbi.de/protocols/competent_cells_electro_v1_0.htm). A 5 mL LB culture of DH5-α was grown overnight and then used to inoculate 500 mL LB. The culture was grown to an optical density 600 nm (OD_{600}) of between 0.4 and 0.5, after which cells were pelleted by centrifugation at 4000 RCF. The pellet was rinsed, re-suspended with autoclaved distilled water, and re-pelleted a total of 3 times at 4000 RCF. After the three rinses, the cells were re-suspended in 100 mL of 10% glycerol. Cells were then pelleted and re-suspended in 2.5-5 mL of 10% glycerol. 80 µL aliquots of cell suspension were dispensed into 150 ul tubes, and frozen in a -80^{o}C freezer for storage. The 80 µL aliquots were then thawed and used for individual electroporation reactions as required.

2.2.2 *Agrobacterium tumefaciens*

GV3101 pPM6000 *Agrobacterium tumefaciens* was streaked out from a glycerol stock onto Lysogeny Broth (LB) with 25 µg/ mL Rifampicin and 25 µg/ mL Gentamycin plates and grown at

28ºC for 2 days. A single GV3101 colony was then grown in 25 mL NaCl free LB for 24 hours to create a starter culture. The next day, the 25 mL starter culture was added to 250 mL of NaCl free LB and allowed to grow until the OD_{600} was between 1 and 1.5. Cells were then placed on ice for 20 minutes, followed by centrifugation at 4000 RCF for 15 minutes. After centrifugation, the supernatant was discarded and cells were re-suspended in 250 mL of autoclaved distilled water. The rinsing and resuspension in distilled water was repeated three times. After the rinses, cells were re-suspended in 25 mL of ice-cold 10% glycerol. Cells were then centrifuged for 10 minutes at 3000 RCF, re-suspended in 1 mL 10% glycerol, divided into 80 µL aliquots, and frozen at -80ºC for future use. For individual electroporation reactions the full 80 µL aliquots were used.

2.3 Construction of FORKED-LIKE Promoter B-glucuronidase Fusion Constructs

2.3.1 pFl1:GUS and pFL2:GUS

The promoters of *FL1* (At5g43870; 3.9 kb of the promoter, including the 5'UTR, the start codon and an additional 3 nucleotides within the ORF) and *FL2* (At3g22810; 3.6 kb of the promoter, together with the 5'UTR, the start codon and an additional 10 nucleotides within the ORF) were previously amplified from plant genomic DNA by PCR using the FL1:cjet and FL2:cjet primers (Table 1). The PCR products were ligated into the plasmid pJet1.2/blunt (Thermofisher) yielding pFL1:cJET and pFL2:cJET respectively (Wilton, unpublished results). The pFL1:cJET and pFL2:cJET plasmids were digested with XmaI and SalI respectively, the excised gene promoter fragments of the restriction endonuclease digestions were gel extracted according to manufacturer's instructions using QIAquick Gel Extraction Kit (Qiagen). For all pBI101.3 ligations, pBI101.3 was digested with restriction enzymes (XmaI for the pFL1 insert and SalI for the pFL2 insert) and treated with Antarctic phosphatase (NEB) according to the manufacturer's protocol. The ligation of pFL1 and pFL3 into pBI101.3 was then done with a 3:1 molar ratio of insert to vector with T4 DNA Ligase (NEB) and ligation buffer in a 20 µL reaction, and left

overnight at room temperature (20-24 ºC). 5 ul of ligation mixture was electroporated into electro-competent *E. coli*. Transformants were screened on LB 50 μg/mL Kanamycin (Kan_{50}), and single colonies were screened by restriction digestion with EcoRI (NEB), BamHI (NEB) and the enzymes used for the individual promoter insertions. Following identification by restriction digestion of plasmids carrying insertion of the correct size, plasmids were sequenced using the pBI-Seq F+R primers (Table 1) by the McGill University and Génome Québec Innovation Centre using Sanger sequencing according to their sequencing guidelines.

2.3.2 pFL2x:GUS

Unfortunately, the pBI101.3 vector contains a translation termination codon in frame with the SalI site (Figure 2.1). Thus, our original pFL2:GUS vector included a termination codon between the translation initiation site of pFL2 and the translation initiation site of B-glucuronidase (GUS). Because we did not know the consequences of this termination codon to the translation of the GUS protein, I generated a second *FL2* promoter construct (3.6 kb of the promoter, together with the 5'UTR, the start codon and 9 nucleotides of the ORF) that replaced the 3' SalI site of the *FL2* promoter with an XmaI site that inserts downstream of the stop codon in pBI101.3 (Figure 2.1). The *FL2* promoter was amplified from pFL2:cjet using the pFL2x Primers (Table 1). The unpurified PCR product was ligated into pJet1.2 according to the manufacturer's protocols (Thermofisher) to make pFL2x:cjet. Then pFL2x:cjet was digested with SalI and XmaI restriction enzymes and ligated into pBI101.3 (see Section 2.3.1). Since no purification step was done for the digestion, either the pFL2x promoter or the pJet1.2 back bone could be ligated into pBI101.3. Positive *E. coli* transformants of pFL2x:GUS and pFL3:GUS were screened by Kan_{50} selection. Kanamycin resistant colonies were replica plated on 100 μg/mL ampicillin (amp_{100}), and all colonies resistant to ampicillin were discarded, as these likely harboured plasmids into which the pJet1.2 backbone had ligated. To screen for the pFL2x promoter, transformants were first plated

on LB_{kan50} and then replica plated on LB_{amp100}. Colonies that only grew on LB_{kan50} were digested with BamHI and EcoRI as well as a combination of SalI and XmaI, the plasmids showing correct band sizes by gel electrophoresis where then sequenced using the pBI-Seq F+R primers (Table 1).

2.3.3 pFL3:GUS

Several attempts were made to amplify different regions upstream of the *FL3* (AT4g14740) translational start site (primers listed in Table 1). Unfortunately, none yielded sufficient specific amplicon for ligation. Finally, the At4g14740 (*FL3*) promoter (2.3 kb ending at the transcription start site; TSS) was synthesised by Biobasic into pBluescript 1.2 to make the pBlue:FL3 plasmid. pBlue:FL3 was subsequently digested with XbaI and XmaI and ligated into pBI101.3 (see section 2.3.1), followed by screening by replica plating as done for *pFL2x:GUS* (see Section 2.3.2).

2.4 pFKD1:GUS Mutagenesis

Identification of putative *cis*-regulatory elements of the *FKD1* promoter was done using AGRIS (Davuluri et al., 2003; Yilmaz et al., 2011), which identified auxin (AuxRE: tgtctc; Ulmasov et al., 1999), Drought (DRE-like; aaccgacaa; Chen et al., 2002), and ABA responsive elements (ABRE-like: tacgtgta; Shinozaki and Yamaguchi-Shinozaki, 2000). Primers were designed to introduce a point mutation (mutation sites highlighted in Table 2) into either the DRE-like (aaccgacaa ->aaccg**T**caa; producing pFKD1-1208A>T:GUS), the ABRE-like (tacgtg ->tacg**A**g; producing pFKD1-1222T>A:GUS), or an AuxRE element (explained below) which, based on previous transcription factor binding assays reduced transcription factor binding efficiency (AuxRE, Ulmasov et al., 1999; ABRE, Shen et al., 2004; DRE, Sakuma et al., 2002). The multiple mutants pFKD1-1222T>A-1208A>T:GUS (pFKD1-DRAB:GUS) and pFKD1-1410T>A-844A>T-482A>T:GUS (pFKD1-A3:GUS) are explained in more detail below. The

forward and reverse primers for an individual mutagenesis reaction were designed with a complementary region of 15-20 nucleotides (required for homologous recombination to circularize the linear amplicon) containing the mutation site and an additional extension region of 10 bp to increase the efficiency of template binding (Xia et al., 2015). Mutagenesis PCR was done with FastPfu (TRANS) and 200 nM forward and reverse primers (Table 2), using an Initial denaturation (95 ^{o}C for 5 minutes), followed by amplification (25 cycles of denaturation at 94^{o}C for 20 seconds, annealing for 20 seconds; see Table 2 for primer specific temperatures, and 72^{o}C elongation for 4 minutes), and a final extension of 72 ^{o}C for 10 minutes to complete any incomplete amplicons. PCR reactions were done with FastPfu (TRANS) and 200 nM forward and reverse primers (Table 2). Amplification of the mutagenized product was confirmed by gel electrophoresis on a 1% agarose gel at 150 volts in a 15 cm tank for 20 minutes.

After amplification was confirmed by TAE gel electrophoresis, the PCR product was treated with 1 µL of DMT (a proprietary methyl group requiring restriction endonuclease similar to DpnI; TRANS®) for 1 hour at 37 ^{o}C. Following the DMT treatment, 5 µL of the DMT treated PCR product was added to 50 µL of DMT chemically competent cells, which were incubated on ice for 30 minutes. Cells were then heat shocked at 42 ^{o}C for 45 seconds and placed on ice for 2 minutes. Afterwards, 250 µL of LB was added to the cells and cells were shaken at 200 rpm at 37 ^{o}C for 1 hour. Cells were then plated on LB_{kan50} plates for selection. Single colonies were selected and plasmids isolated using the QuickPure Plasmid Minikit (CWBIO) with positives being detected by sequencing with the FKD1-seq primers (Table 1) to verify mutagenesis.

To produce the multiple mutant constructs such as the triple AuxRE mutant (pFKD1-A3:GUS) and the ABRE-like and DRE-like double mutant (pFKD1-DRAB:GUS), sequential mutagenesis of the plasmid had to be done. The construction of pFKD1-A3:GUS started with mutating pFKD1:GUS with the FKD1-AuxRE1 primers (Table 2; tgtctc -> tgtc**A**c mutation), this product (pFKD1-1410T>A:GUS) was then transformed into *E. coli*, and plasmid re-isolated

resulting in a single distal AuxRE mutant (pFKD1-1410T>A:GUS). The single AuxRE mutant plasmid was then used for another PCR with the FKD1-AuxRE2 primers (Table 2; reverse oriented AuxRE: gagaca -> g**T**gaca) the product (pFKD1-1410T>A-844A>T:GUS) was isolated and transformed into *E.* coli producing a pFKD1:GUS double AuxRE mutant. Finally the pFKD1:GUS double AuxRE plasmid was mutated with the FKD1-AuxRE3 primers (Table 2; reverse oriented AuxRE: gagaca -> g**T**gaca) this resulted in the pFKD1:GUS triple AuxRE mutant (pFKD1-1410T>A-844A>T-435A>T:GUS, or pFKD1-A3:GUS) which was then transformed into *E. coli,* and sequenced to verify the correct mutations. The FKD1-DRE+ABRE mutations were done using the ABRE-like mutagenized pFKD1:GUS (pFKD1—1222T>A:GUS) as a template and amplified with the FKD1-DRE+ABRE primers (Table 2) producing the ABRE-like DRE-like pFKD1:GUS double mutant (pFKD1-DRAB:GUS). It is worth noting that *E. coli* transformed with the FKD1-DRAB:GUS mutant required 1.5-2 days to show positive colonies which were verified by sequencing (Table 1).

2.5 Plant Transformations

For plant transformation by floral dip, wild type Arabidopsis seed (Columbia genotype) were sown on soil (3:1 soilless potting mix: vermiculite), stratified for 4 days at 4 ^{o}C, then transferred to a growth chamber at 22 ^{o}C until the first siliques began to form (~23-27 Days after germination; DAG). A single colony of transformed GV3101 pPM6000 agrobacterium was used to inoculate a 5 mL LB culture, which was grown for 16-24 hours with appropriate antibiotics. The starter culture was then used to inoculate 200 mL LB with antibiotics. This 200 mL LB culture was grown until an OD_{600} of ~1.0 was reached. The cultures were then spun at 4000 RCF for 15 minutes and re-suspended in 200 mL of fresh LB with 5% w/v glucose. After re-suspension, 0.05% silwet was added. Plants were then dipped in the Agrobacterium solution for 20-30 seconds. After allowing excess Agrobacterium to drip off, plants were covered in saran

wrap and a black bag to maintain humidity and protect from light and placed into the growth chamber overnight. The bag was removed the next morning and plants gradually introduced to chamber conditions by poking holes in the saran wrap for the next 2 days.

For all plant transformations, transformed T_1 plants were screened at 10 DAG after growth on AT plates with AT_{kan50} (pBI101.3 based plasmids) or at 8 DAG after growth on soil and spraying with 0.001% Liberty at 7 DAG (pFKD1:GUS mutagenized plasmids). Self-fertilization generated the T_2 generation, which was re-screened for resistance, and allowed to self-fertilize to produce a segregating population (3:1 resistant to sensitive). A line with a representative GUS expression pattern was selected from at least 10 independent T_1 lines following staining (see below) of the T_1 populations and used to develop a homozygous line. Unfortunately, due to time constraints, I was unable to generate lines homozygous for the pFKD1:GUS mutagenized plasmids. Thus, I was unable to analyse the altered expression patterns resulting from these mutations.

2.6 Hormone treatment and GUS-Staining

2.6.1 Hormone Treatments

Plants used for GUS staining and in response to hormones and environmental stresses were treated in the following ways. For 2,4-Dichlorophenoxyacetic acid (2,4-D), ABA, Mannitol, or NaCl treatments, lines were seeded on AT media plates (Ruegger et al., 1998) and stratified for 3-4 days at 4^{o}C in the dark. Seed were transferred to growth chambers, and grown at 22 ^{o}C in continuous light (~130 μmol photons per m^2 per second) until 5 DAG when seedlings were transferred to liquid AT containing Auxin (0.1%DMSO, 0.1 μM or 1 μM), ABA (0.1% Methanol, 0.1 μM, 0.5 μM, or 1 μM), mannitol (At, 150 mM or 300 mM) or NaCl (AT, 100 mM or 300 mM) for 16 hours shaken at 120 rpm in a growth chamber and then GUS stained.

2.6.2 Gus Staining and Clearing

Arabidopsis seedlings (n ≥20) were transferred from plates or treatments to 1.5 mL microfuge tubes with 1 mL 90% acetone on ice for 1 hour, and subsequently washed two times with 50 mM $NaPO_4$ for 5 minutes. The $NaPO_4$ buffer was then removed and X-Gluc solution (50 mM $NaPO_4$, 3 mM $K_3Fe_3(CN)_6$, 10 mM Ethylenediaminetetraacetic acid, 0.1% (v/v) Nonidet P40, 0.75 mg/ mL X-gluc) was added. Seedlings were placed under a vacuum of 9 PSI during staining at room temperature. After staining, seedlings were rinsed with 70% ethanol 4 times, and cleared with 8:2:1 chloral hydrate: glycerol: distilled water for 3-5 days. Following clearing, seedlings were mounted on slides and pictures take on a Nikon Eclipse E600 microscope using a Nikon Coolpix 990 camera.

Table 1: Primers used for the construction of the *FL*-gene reporter GUS constructs and their verification. Highlighted sequences indicate restriction cut sites. T_A indicates the annealing temperature used for the primer pair.

Name	Forward 5'to 3'	Reverse 5' to 3'	T_A
pBI101_3 Seq	CTTCCGGCTCGTATGT TGTG	ATCCAGACTGAATGCCC ACA	N/A
FKD1-Seq	TGGTTGTGGTTGCTCT TCTTT	ACGGATTAGGTGCTGAA ATTTGG	N/A
FL1:cjet	AATGGCCCGGGGATT GTTAACTTGAGTAGC TGC	TGCTCGCCCGGGATCCA TTATCTAATGAAAGAG	60 ºC
FL2:cjet	ACATCGTCGACCAAA ATATGTTTAAGTCAT CC	TAATCGTCGACCTGGTT TCTCCATTTTACAGAG	62 ºC
FL2x-GUS	ACATCGTCGACCAAA ATATGTTTAAGTCAT CC	AATTACCCGGGTGGTTT CTCCATTTTACAGAG	60 ºC
A4-3kb-Blunt	ATC TGA GGG TTG GGT GGT GT	ATC GGG GAT TGG ACT GTG GG	68 ºC
A4F-3kbXmaI+BamHI	ATT A GGATCC AA ATC GGG GAT TGG ACT GTG	GAA G CCCGGG TC CAT GTC GGA ACC ATG AG	68 ºC
A4-Promo no 5' UTR	ATA GGATCC ATC CAC CCA TCC GCA TAA CC	ATA CCCGGG GGA AGT GAA AGG TTG TCA ATG GGG A	68 ºC
At4_2.9kb	ATT A GGATCC TG TGG AGT CCC AAC ACA TCC	ATT A GGATCC TG TGG AGT CCC AAC ACA TCC	67 ºC

Table 2: Primers used to generate the pFKD1:GUS mutagenesis constructs. Bold capitalized nucleotides indicate the mutation sites mutated sites, while underlined regions show overlapping regions. T_A indicates the annealing temperature used for the primer pair.

Name	Forward 5' to 3'	Reverse 5' to 3'	**T_A**
FKD1-AuxRE1	cctgttgtgtc**A**cccctgttgctgttcc	caggggg**T**gacacaacaggaacataaactg	58 ºC
FKD1-AuxRE2	ggaataatcagag**T**gacaaaatgactagt	tgtc**A**ctctgattattcctttgccttgc	54 ºC
FKD1-AuxRE3	g**T**gacagagagaagaaggtgacgtaaggg	ccttcttctctctgtc**A**cttttccacttc	57 ºC
FKD1-DRE	aaccg**T**caacagggtttagctcgcaagtc	aaccctgttg**A**cggtttgatctacacgt	59 ºC
FKD1-ABRE	**A**gtagatcaaaccgacaacagggtttag	gttgtcggtttgatctac**T**cgtacaaa	55 ºC
FKD1-DRE+ABRE	aaccg**T**caacagggtttagctcgcaagtc	aaccctgttg**A**cggtttgatctac**T**cgt	59 ºC

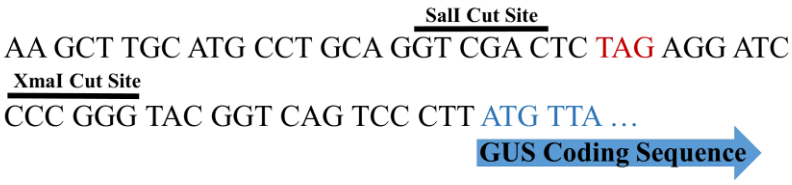

Figure 2.1: Sequence of the pBI101.3 plasmid near the β-Glucouronidase fusion junction. The SalI site was originally used for making the pFL2:GUS promoter reporter construct, however, a downstream in-frame stop codon (red nucleotides) was discovered in the sequence. As such, the promoter reporter plasmid was reconstructed as pFL2x:GUS using the XmaI site downstream of the stop codon.

3.0 Results

3.1 Developmental Analysis of *FL* Gene Promoter:GUS expression

To observe the expression patterns of *FL* gene family members and to test if they have similarspatiotemporal expression, I assessed the expression of *FL1, FL2* and *FL3* by reporter gene fusions. Genomic regions of 3.9 kb (*FL1*), 3.6 kb (*FL2*) and 2.4 kb (*FL3*) upstream of the TSS were ligated to a β-Glucouronidase (GUS) coding sequence to create pFL1:GUS, pFL2:GUS, and pFL3:GUS. Following transformation into wildtype (Col-0) Arabidopsis, analysis of transgene expression in at least 10 independent lines was carried out and a line with representative expression was chosen for further analysis. GUS expression in the representative lines was then assessed in cotyledons, first leaves, and roots from 2 to 6 DAG.

3.2 *pFL1:GUS* expression during seedling development

pFL1:GUS is expressed in cotyledons (Figure 3.1A), root tissues (Figure 3.2B), and developing first leaves (Figure 3.3). In cotyledons, *pFL1:GUS* expression is broad, with low levels of GUS expression throughout cotyledon epidermal cells and more intense expression in the narrow cell files of the provascular tissues (Figure 3.1A). In leaves, *pFL1:GUS* is first visible in the basal and apical tip of the midvein at 4 DAG, and as islands of expression in developing provascular tissue of secondary veins (asterisk, Figure 3.3A). At 5 DAG, *pFL1:GUS* expression occurs throughout the midvein. The expression of *pFL1:GUS* in the secondary veins has, at 5 DAG, extended apically and basally to connect with the mid vein. Additionally, islands of GUS expression of higher order provascular tissues are visible at 5 DAG (asterisk, Figure 3.3B, C). These islands of expression likely extend apically and basally until they reach secondary vein junctions with the mid vein as can be seen at 6 DAG (Figure 3.3D). Higher order veins show a similar pattern to secondary veins, with GUS expression beginning in the center of presumptive veins (asterisks, Figure 3.3D). In roots, *pFL1:GUS* is expressed in the internal cylinder of the root at 6 DAG, with the most intense expression occurring in the zone of cell division near the root apical meristem

and the elongation zone with expression gradually diminishing through the differentiation zone (Figure 3.2B).

3.3 *pFL2:GUS* expression during seedling development

pFL2:GUS is expressed in cotyledon, leaf, and root tissues during plant development. For the analysis of *pFL2:GUS* a segregating population was used. The segregation ratio of plants with no GUS expression (46 plants), to weak expression (75 plants), to strong expression (32 plants) of *pFL2:GUS* was analyzed by a Chi square test to confirm that the results did not significantly differ from the expected 1:2:1 ratio (Chi square $p = 0.27$, $df = 2$). Strong GUS expressing *pFL2:GUS* seedlings were selected for analysis as they were most likely to be homozygous for the pFL2:GUS insertion. The cotyledon expression of *pFL2:GUS* occurs in the vasculature, with the highest levels of GUS expression tending to occur at or near points of vein meeting (Figure 3.1B). The expression of *pFL2:GUS* in leaf venation begins in the secondary veins near where the apical midvein and the secondary veins meet (asterisk, Figure 3.4C, D). At later developmental stages, the expression of *pFL2:GUS* occurs throughout leaves with higher expression often occurring at or near points of vein meeting (asterisk, Figure 3.4E). The venation expression of *pFL2:GUS* is relatively weak and may be transient in nature as it occurs sporadically in leaf venation, without a consistent localization pattern in venation (Figure 3.4E). During early development, strong expression of *pFL2:GUS* occurs in two regions of about 1-4 epidermal cells in the basal half of the leaf, about midway between leaf margin and midvein (arrow, Figure 3.4A, B). At later developmental stages the expression at the basal half of the leaf intensifies (arrow, Figure 3.4B) and expands apically to include parts of the leaf margin (arrow, Figure3. 4C). This basal expression domain becomes most intense at the blade petiole boundary (arrow, 3.4C, D). *pFL2:GUS* expression also occurs in the leaf margin and nearby epidermal cells (Figure 3.4A-E). At early stages of leaf development, before blade and petiole are distinguishable (Figure 3.4A, B),

expression occurs in the margin from the base of the leaf to about halfway up the leaf. At later developmental stages, the leaf margin and basal expression domains merge and extend into the petiole (Figure 3.4C-E). Weak root expression of *pFL2:GUS* occurs (in the internal region of the root), in the distal meristematic zone and the zone of elongation (Figure 3.2C).

3.4 *pFL3:GUS* expression during seedling development

The expression of *pFL3:GUS* is initiated later than the other FL genes in cotyledons and leaves and is not visible in root tissues. In cotyledons, *pFL3:GUS* is expressed all along the cotyledon margin at 6 DAG (Figure 3.1C). In leaves, *pFL3:GUS* expression begins to occur at 5 DAG in apical trichomes and subsidiary cells (Figure 3.5B). At 6 DAG, the expression of *pFL3:GUS* includes more basal trichomes and the apical leaf margin (Figure 3.5C). Additionally at 6 DAG, faint expression in leaf epidermal cells can be seen. No root expression of *pFL3:GUS* was visible after 24 hours of staining, suggesting that FL3, uniquely amongst for the group I *FL* gene family members, is not expressed in roots (Figure 3.2D).

3.5 *in silico* promoter analysis of Group I *FL*- genes

Initially, *in silico* analysis of the *FL* gene family was done to predict putative *cis*-regulatory elements in their promoters that may be driving gene expression. For the analysis of *FL*-gene family promoters AGRIS was used. Promoter analysis, using AGRIS (Yilmaz et al., 2011; Palaniswamy et al., 2006; Davuluri et al., 2003), revealed several common promoter themes including presence of ABA response elements (ABRE/ABRE-like and ABF elements), Auxin response elements (AuxRE), and circadian clock related elements such as circadian clock associated (CCA) which are affected by light levels through PIFs (Nomoto et al., 2012; Viczián et al., 2005) and evening elements (EE).

FKD1 contains AuxRE, ABRE-like, and DRE-like element binding sites in its promoter region. The three putative auxin response elements are dispersed throughout the *FKD1* promoter (705, 1068, 1637 bp upstream of TSS). Interestingly, the ABRE-like and DRE-like elements (1449 and 1436 bp upstream of TSS; Figure 3.6) are closely linked within the *FKD1* promoter. A single ABRE-like element is not capable of responding to exogenous ABA or drought response, on its own, but requires a coupling element such as a DRE-like (Narusaka et al., 2003). Previously, a 5 bp gap was shown to allow ABRE-element coupling with an EE element (Mikkelsen and Thomashow, 2009).

The group I *FL* genes have a number of elements in common with *FKD1*. *FL1* contains several cis regulatory sites including AuxRE (1013, 1213, and 2142 bp from the TSS), ABRE (166, 901), and CCA elements. CCA is a circadian clock associated protein for which *FL1* has 4 putative binding sites (69, 2094, 2179, and 2201; Figure 3.6). While *FL2* has a single putative AUXRE element that occurs 2093 bp from the TSS, and a cluster of three CCA1 elements are clustered within a region of about 200 bp (1149, 1280, and 1339 bp from the TSS; Figure 3.6). *FL3* has putative AuxRE (2271 upstream TSS) and DRE-like (1061 upstream TSS) elements, and is unique among the *FL* genes in that it has several EE (393, 2343 upstream TSS; Figure 3.6).

3.6 Treatment of *pFKD1:GUS* with 2,4-D, ABA, NaCl and Mannitol

To confirm the effects of auxin on *pFKD1:GUS* expression during leaf and root development I exposed *pFKD1:GUS* seedlings to a short term 2,4-D treatment. The importance of AuxRE elements to FKD1 expression was implied by increased *pFKD1:GUS* expression in response to exogenous 2,4-D and the reduced expression of *pFKD1:GUS* in *monopterous* (*mp*/*arf*5) mutants. Additionally, *auxin resistant1-3* (*axr 1-3)* seedlings that have reduced auxin response, showed reductions in *FKD1* expression, assessed at 5 DAG by either *pFKD1-GUS* or RT-qPCR (Hou et al., 2010). The changes to *pFKD1:GUS* expression in response to exogenous 2,4-D observed by

Hou and colleagues (2010), were following growth of seedlings for 3-5 DAG on 1 μM 2,4-D, which causes developmental abnormalities including reduced leaf expansion, changes to vein pattern, and reductions in root elongation. To avoid these developmental abnormalities and assess short term change to *pFKD1:GUS* expression induced by auxin, I germinated and grew *pFKD1:GUS* on AT media until 5 DAG and then transferred the plants to liquid AT media containing 0.1% DMSO (control), 1 μM 2,4-D, or 10 μM 2,4-D for 16 hours. Short term treatment with 1 μM or 10 μM 2,4-D increase *pFKD1:GUS* expression throughout the leaf compared to the untreated control (Figure 3.7B). The increased *pFKD1:GUS* is similar to previous observations (Hou et al., 2010), but is not accompanied by obvious leaf developmental defects. Interestingly, compared to the expression following 1 μM 2,4-D treatment, expression at 10 μM 2, 4-D is reduced throughout the leaf but most noticeably at the leaf apex, (Figure 3.7C). In roots, *pFKD1:GUS* expression is not visible in either untreated or 1 μM 2,4-D, but is visible in the elongation zone of roots treated with 10 μM 2,4-D (Figure 3.8C). These results suggest that in both roots and leaves, expression of the *FKD1* gene is increased by auxin with variable sensitivities.

To test the effects of ABA on *pFKD1:GUS* expression, seedlings were exposed to short term ABA treatment. In response to 16 hour treatment with exogenous ABA, *pFKD1:GUS* expression in both leaves and roots decreased. Low levels of exogenous ABA (0.1 μM) caused noticeably decreased *pFKD1:GUS* expression levels throughout the leaf and root (Figure 3.9B; 3.10B), and higher concentrations of ABA (0.5 or 1.0 μM) decreased *pFKD1:GUS* leaf and root expression to the point where it was no longer visible (Figure 3.9C, D; 3.10C, D). These results indicate that the addition of ABA-reduces *pFKD1:GUS* expression in leaves and roots.

I next tested if *pFKD1:GUS* responds to osmotic and salt stress, as the presence of a close DRE-like and ABRE-like element in the promoters indicated that *pFKD1:GUS* may respond differently to drought than ABA alone. *pFKD1:GUS* seedlings were transferred to liquid AT

culture containing either mannitol to induce osmotic stress or NaCl, to induce salt stress for 16 hours. In response to mannitol and NaCl treatments, *pFKD1:GUS* expression in leaves generally decreased, whereas expression in roots generally increased. Relative to untreated leaves, treatment with 150 mM mannitol decreased *pFKD1:GUS* leaf expression throughout the leaf, with the 300 mM mannitol treatment not inducing a visible change in *pFKD1:GUS* leaf expression compared to the untreated control (Figure 3.11B, C). In leaves, particularly in the basal half, both the 100 mM and 150 mM NaCl treatments reduced *pFKD1:GUS* expression (Figure 3.11D, E). Compared to leaves, roots showed a different pattern of *pFKD1:GUS* response to mannitol and NaCl (Figure 3.12). Treatment with 150 mM mannitol did not affect *pFKD1:GUS* root expression, while the 300 mM mannitol treatment resulted in more intense and broader *pFKD1:GUS* expression throughout the root (Figure 3.12B, C). The 100 mM NaCl treatment did not affect *pFKD1:GUS* root expression, while 150 mM NaCl treatment caused increased expression limited to the zone of elongation (Figure 3.12D, E).

3.7 Treatment of *pFL1:GUS* with 2,4-D, ABA, NaCl and Mannitol

To test the significance of the AuxRE elements in the *pFL1:GUS* promoter, I treated *pFL1:GUS* seedlings with 2,4-D. In 6 DAG (5 DAG on plates and 16 hours in liquid AT) leaves, *pFL1:GUS* expression increased slightly in response to 16 hour treatment with all concentrations of 2,4-D (Figure 3.13). The expression of *pFL1:GUS* is strongest in the mid vein of all the treatments, and expression increases with increasing 2,4-D concentration. Treatment with the highest concentration of 2,4-D tested (10 μM) also resulted in expression in the secondary veins (Figure 3.13C) . In response to the treatment with 2,4-D, *pFL1:GUS* root expression extended upwards, resulting in stronger *pFL1:GUS* expression in the elongation zone of the root, with no noticeable changes in expression intensity in the meristematic zone (Figure 3.14).

To determine if *pFL1:GUS* is responding to ABA, I treated *pFL1:GUS* seedlings with ABA. In response to 16 hour ABA treatment, *pFL1:GUS* showed concentration dependent decreases in expression in leaves and roots. Treatment with 0.1 μM and 0.5 μM ABA decreased *pFL1:GUS* leaf expression, most noticeably in the second order provascular tissue (Figure 3.15B, C). Treatment with 1.0 μM ABA substantially reduced all *pFL1:GUS* leaf expression (Figure 3.15D). In roots, 0.1 μM and 0.5 μM ABA resulted in reduced expression in the differentiation and elongation zones. At 0.5 μM ABA, expression is restricted to the distal meristematic zone (Figure 3.16B, C). As in leaves, the expression of *pFL1:GUS* expression is absent from the root following treatment with 1.0 μM ABA (Figure 3.16D).

The lack of predicted DRE or drought related coupling elements indicated that *pFL1:GUS* was unlikely to be regulated by salt and osmotic stress, likely showing a different stress response than *pFKD1:GUS*. To confirm that *pFKD1:GUS* and *pFL1:GUS* show different responses to salt and osmotic stress I exposed *pFKD1:GUS* and *pFL1:GUS* seedlings to 16 hour mannitol (osmotic) and NaCl (salt) treatments in liquid AT media. In leaves, all concentrations of mannitol or NaCl decreased *pFL1:GUS* expression, with NaCl causing particularly pronounced decreases in GUS expression (Figure 3.17). In roots, the 150 mM Mannitol treatment had no noticeable effects on *pFL1:GUS* expression, while the 300 mM mannitol treatment reduced the intensity of *pFL1:GUS* expression in the meristematic zone without changing expression in the elongation zone. Both NaCl treatments decreased *pFL1:GUS* expression in roots, with 100 mM NaCl limiting pFL1:GUS expression to the distal meristematic zone (Figure 3.18D), while the 150 mM NaCl treatment almost entirely abolished *pFL1:GUS* expression (Figure 3.18E).

3.8 pFKD1:GUS Mutagenesis

The mutagenesis of the *FKD1* promoter was done based on the AGRIS *cis*-regulatory promoter analysis. Previous results have indicated that *FKD1* expression is regulated by auxin (Hou et al.,

2010) and responds to ABA treatment (Veenendaal unpublished results, Li unpublished results). Putative related *cis*-regulatory elements that were identified in the promoter analysis were mutated to remove functionality based on previous transcription factor binding assays (AuxRE, Ulmasov et al., 1999; ABRE, Shen et al., 2004; DRE, Sakuma et al., 2002). I was able to generate T_1 mutants of *pFKD1-A3:GUS, pFKD1-ABRE:GUS, pFKD1-DRE:GUS* and the *pFKD1-DRAB:GUS*. However, these plants need to be screened before further use in comparison of their effects on the regulation of *pFKD1:GUS* in response to 2,4-D, ABA, Mannitol, and NaCl.

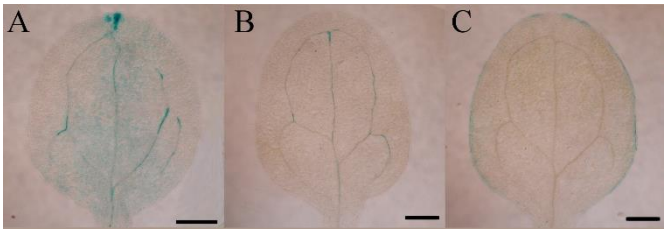

Figure 3.1: Expression of *FL* genes in 6 DAG cotyledons. *pFL1:GUS* (A), *pFL2:GUS* (B), or *pFL3:GUS* (C) expressing seedlings were grown on AT plates. Seedlings were stained in GUS buffer for 24 hours, cleared and cotyledons mounted on slides (scale bar= 0.3 μm).

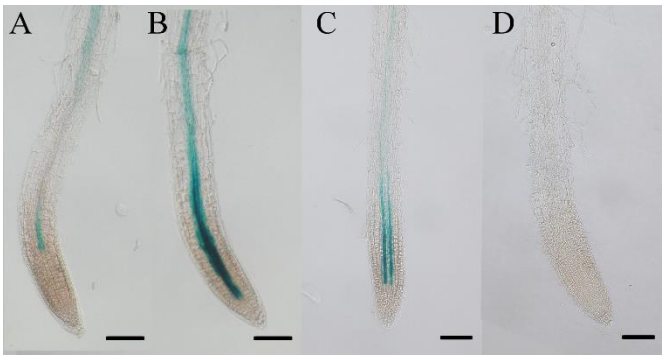

Figure 3.2: Expression of *FL* genes in 6 DAG roots. *pFKD1:GUS* (A), *pFL1:GUS* (B), *pFL2:GUS* (C), or *pFL3:GUS* (D) expressing seedlings were grown on AT plates. Seedlings were stained in GUS buffer for 2 (*pFKD1:GUS*), 6 (*pFL1:GUS*), or 24 hours (*pFL2:GUS* and *pFL3:GUS*) cleared and roots mounted on slides scale bar= 0.1 μm).

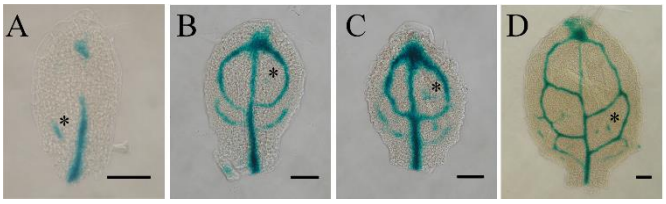

Figure 3.3: Expression of *pFL1:GUS* during first leaf development. *pFL1:GUS* expressing seedlings were grown on AT plates and harvested at 4 DAG (A), 5 DAG (B), 6 DAG (C), or 7 DAG (D). Seedlings were stained in GUS buffer for 6 hours, cleared and first leaves mounted on slides. Asterisks indicate *pFL1:GUS* expression in the middle of a provascular strand (scale bar= 0.1 μm).

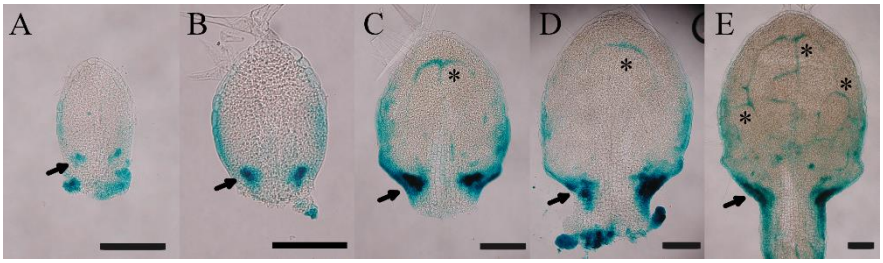

Figure 3.4: Expression of *pFL2:GUS* during first leaf development. A population segregating for *pFL2:GUS* expressing seedlings were grown on AT plates and harvested at 3 DAG (A), 4 DAG (B), 5 DAG (C), 6 DAG (D), or 7 DAG (E). Seedlings were stained in GUS buffer for 6 hours, cleared and first leaves from the strongest staining seedlings mounted on slides (arrows indicate the basal expression domain; asterisks indicate high expression where venation meets; scale bar= 0.1 μm).

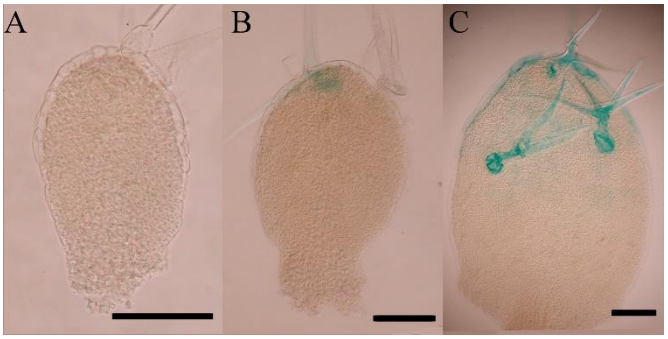

Figure 3.5: Expression of *pFL3:GUS* during first leaf development. *pFL3:GUS* expressing seedlings were grown on AT plates and harvested at 4 DAG (A), 5 DAG (B), or 6 DAG (C). Seedlings were stained in GUS buffer for 24 hours, cleared, and first leaves mounted on slides (scale bar= 0.1 μm).

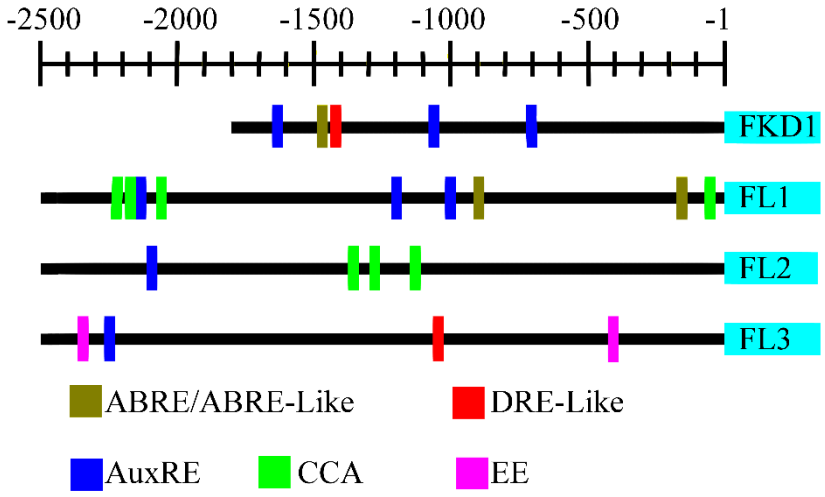

Figure 3.6: Diagram showing putative drought, ABA, auxin, and circadian clock related elements in the promoters of the group I *FL* gene family upstream of the transcription start site as predicted using AGRIS (Yilmaz et al., 2011; Palaniswamy et al., 2006; Davuluri et al., 2003). Abbreviations: ABRE (ABA response element), DRE (Drought responsive element), AuxRE (Auxin Response Element), CCA (Circadian Clock Associated), EE (Evening Elements).

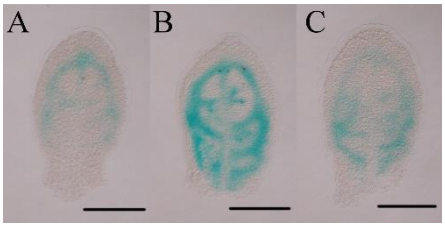

Figure 3.7: 2,4-D treatment alters *pFKD1:GUS* expression in leaves. *pFKD1:GUS* seedlings were germinated and grown for 5 days on AT plates after which they were transferred to liquid AT with 0.1% DMSO (A), 1 um 2,4-D (B) or 10 uM 2,4-D (C). After 16 hours, seedlings were stained in GUS buffer for 2 hours, after which they were cleared, and first leaves mounted on slides (scale bar= 0.1 μm).

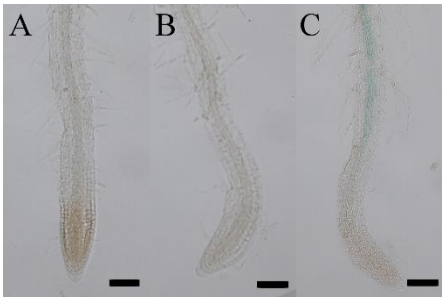

Figure 3.8: 2,4-D treatment alters *pFKD1:GUS* expression in roots. *pFKD1:GUS* seedlings were germinated and grown for 5 days on AT plates after which they were transferred to liquid AT with 0.1% DMSO (A), 1.0 uM 2,4-D (B) or 10 uM 2,4-D (C). After 16 hours, seedlings were stained in GUS buffer for 2 hours, after which they were cleared, and roots mounted on slides (scale bar= 0.1 μm).

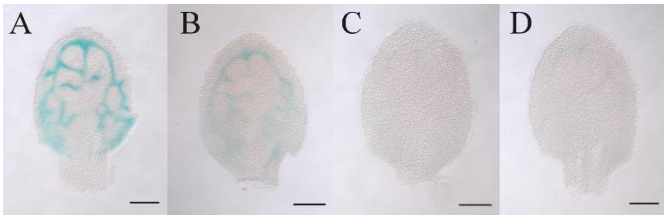

Figure 3.9: ABA treatment alters *pFKD1:GUS* expression in leaves. *pFKD1:GUS* seedlings were germinated and grown for 5 days on AT plates after which they were transferred to liquid AT with 0.1% methanol (A), 0.1 uM ABA (B), 0.5 uM ABA (C), or 1.0 μM ABA (D). After 16 hours, seedlings were stained in GUS buffer for 2 hours, after which they were cleared and first leaves mounted on slides (scale bar= 0.1 μm).

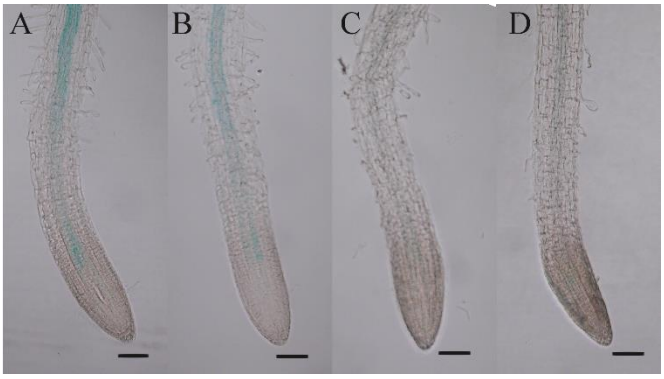

Figure 3.10: ABA treatment alters *pFKD1:GUS* expression in roots. *pFKD1:GUS* seedlings were germinated and grown for 5 days on AT plates after which they were transferred to liquid AT with 0.1% methanol (A), 0.1 uM ABA (B), 0.5 uM ABA (C), or 1.0 μM ABA (D). After 16 hours, seedlings were stained in GUS buffer for 8 hours, after which they were cleared, and roots dissected and mounted on slides (scale bar= 0.1 μm).

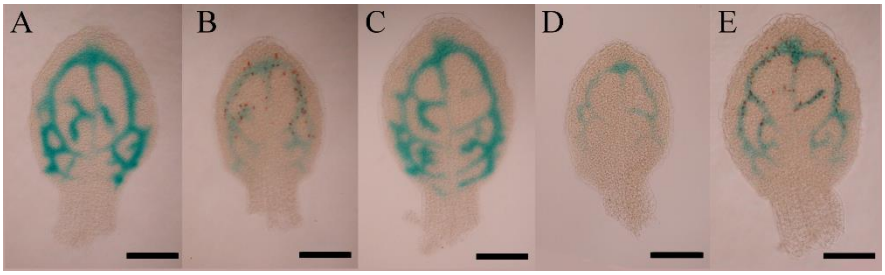

Figure 3.11: Mannitol and NaCl treatment alters *pFKD1:GUS* expression in leaves. *pFKD1:GUS* seedlings were germinated and grown for 5 days on AT plates after which they were transferred to liquid AT (A), liquid AT with 150 mM Mannitol (B), 300 mM Mannitol (C), 100 mM NaCl (D) or 150 mM NaCl (E). After 16 hours, seedlings were stained in GUS buffer for 2 hours, after which they were cleared and first leaves mounted on slides (scale bar = 0.1 μm)

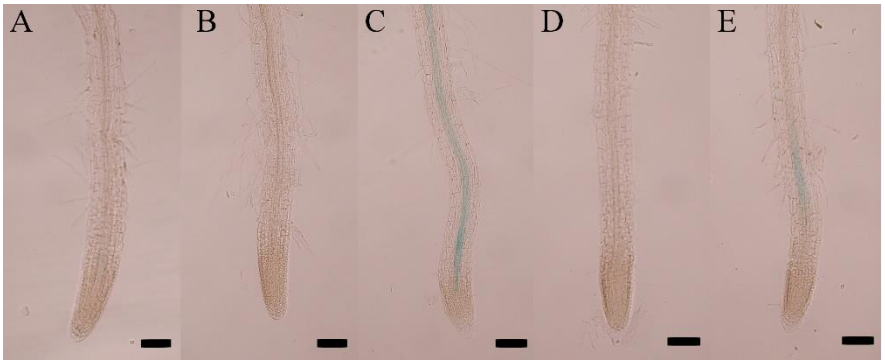

Figure 3.12: Mannitol and NaCl treatment alters *pFKD1:GUS* expression in roots. *pFKD1:GUS* seedlings were germinated and grown for 5 days on AT plates after which they were transferred to liquid AT (A), liquid AT with 150 mM Mannitol (B), 300 mM Mannitol (C), 100 mM NaCl (D) or 150 mM NaCl (E). After 16 hours, seedlings were stained in GUS buffer for 2 hours, after which they were cleared and roots mounted on slides(scale bar= 0.1 μm).

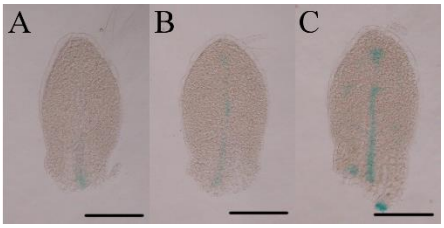

Figure 3.13: 2,4-D treatment alters *pFL1:GUS* expression in leaves. *pFL1:GUS* seedlings were germinated and grown for 5 days on AT plates after which they were transferred to liquid AT with 0.1% DMSO (A), 1 uM 2,4-D (B) or 10 uM 2,4-D (C). After 16 hours, seedlings were stained in GUS buffer for 2 hours, after which they were cleared and first leaves mounted on slides (scale bar= 0.1 μm).

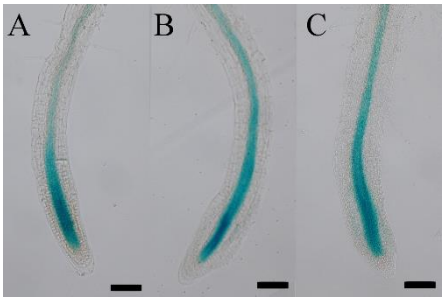

Figure 3.14: 2,4-D treatment alters *pFL1:GUS* in roots. *pFL1:GUS* seedlings were germinated and grown for 5 days on AT plates after which they were transferred to liquid AT with 0.1% DMSO (A), 1 uM 2,4-D (B) or 10 uM 2,4-D (C). After 16 hours, seedlings were stained in GUS buffer for 2 hours, after which they were cleared and first leaves mounted on slides (scale bar= 0.1 μm).

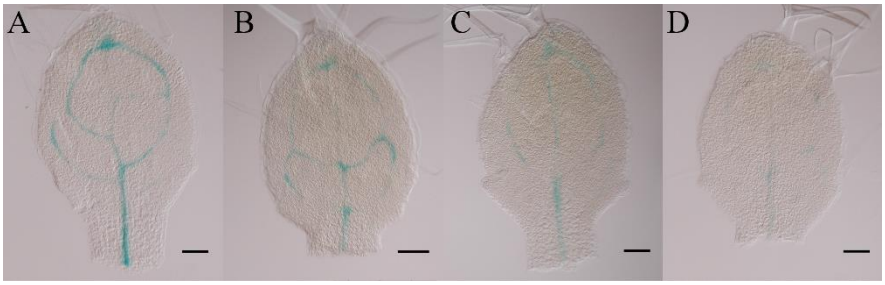

Figure 3.15: ABA treatment alters *pFL1:GUS* expression in leaves. *pFL1:GUS* seedlings were germinated and grown for 5 days on AT plates after which they were transferred to liquid AT with 0.1% methanol (A), 0.1 uM ABA (B), 0.5 uM ABA (C), or 1.0 μM ABA (D). After 16 hours, seedlings were stained in GUS buffer for 2 hours, after which they were cleared and first leaves mounted on slides (scale bar= 0.1 μm).

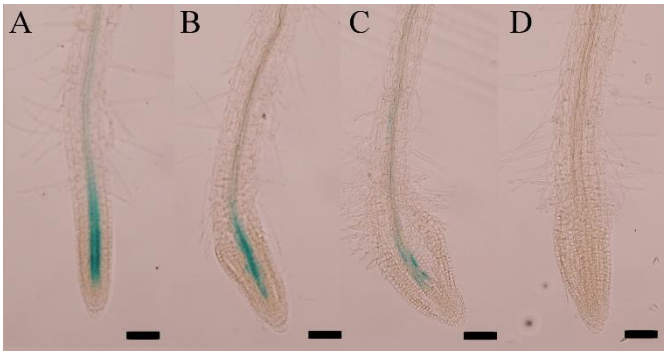

Figure 3.16: ABA treatment alters *pFL1:GUS* expression in roots. *pFL1:GUS* seedlings were germinated and grown for 5 days on AT plates after which they were transferred to liquid AT with 0.1% methanol (A), 0.1 uM ABA (B), 0.5 uM ABA (C), or 1.0 μM ABA (D). After 16 hours, seedlings were stained in GUS buffer for 2 hours, after which they were cleared and roots mounted on slides (scale bar= 0.1 μm).

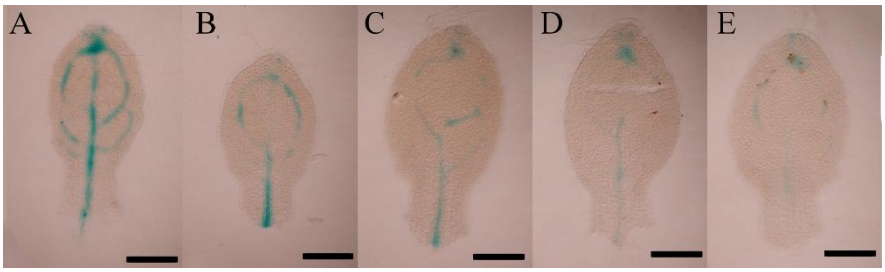

Figure 3.17: Mannitol and NaCl treatment alters *pFL1:GUS* expression in leaves. *pFL1:GUS* seedlings were germinated and grown for 5 days on AT plates after which they were transferred to liquid AT (A), or liquid AT with 150 mM Mannitol (B), 300 mM Mannitol (C), 100 mM NaCl (D), 150 mM NaCl (E). After 16 hours, seedlings were stained in GUS buffer for 2 hours, after which they were cleared and first leaves mounted on slides (scale bar= 0.1 μm).

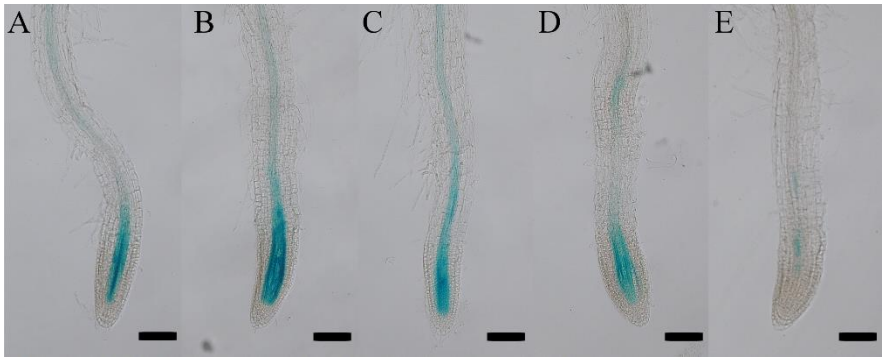

Figure 3.18: Mannitol and NaCl treatment alters *pFL1:GUS* expression in roots. *pFL1:GUS* seedlings were germinated and grown for 5 days on AT plates after which they were transferred to liquid AT (A), or liquid AT with 150 mM Mannitol (B), 300 mM Mannitol (C), 100 mM NaCl (D), 150 mM NaCl (E). After 16 hours, seedlings were stained in GUS buffer for 2 hours, after which they were cleared and first leaves mounted on slides (scale bar= 0.1 μm).

4.0 Discussion

4.1 The Role of *FL* genes in Leaf and Cotyledon Venation

Three of the group I *FL* genes are expressed in vasculature during leaf and cotyledon development, although their expression varies both spatially and temporally. *pFKD1:GUS*, *pFL1:GUS* and *pFL2:GUS* are expressed in cotyledon (Figure 3.1; Hou et al., 2010) and leaf venation (Figure 3.3, 3.4; Hou et al., 2010) with temporal differences in gene expression being observable in the leaf developmental series (Figure 3.3, 3.4). *pFL1:GUS* expression in vascular tissue lags about 2 days behind *pFKD1:GUS* expression. While *pFL2:GUS* expression lags about 3 days behind *pFKD1:GUS* expression based on leaf size and lamina expansion. The initial expression of *pFKD1:GUS* occurs strongly in the region predicting the midvein, with short-lived expression in the provascular tissue of secondary veins at 2-3 DAG as the primordium begins to emerge (Hou et al., 2010). *pFL1:GUS* midvein expression occurs later, at around 4 DAG when the leaf has begun to form a distinct lamina. Strong *pFL1:GUS* expression does not occur until 5-6 DAG when the leaf lamina is noticeably larger than the area that will become the petiole. At a similar time point of 5-6 DAG, *pFKD1:GUS* is already expressed in the pro-vascular tissues that will become tertiary veins, and its midvein expression has begun to decrease (Hou et al., 2010). Interestingly, the timing and localization of *pFL1:GUS* expression from 4-6 DAG correlates well with the narrowing of the PIN expression domains from a group of cells to a cell file as observed by Hou and colleagues (2010). *pFL2:GUS* occurs most noticeably in venation at 7 DAG, though it can be seen earlier in the apical secondary veins (Figure 3.4). The late and limited expression of *pFL2:GUS* may indicate that FL2 has a specialized function in the meeting or maturation of venation. Based on the temporally separated relationship of *pFL1:GUS* and *pFL2:GUS* compared to *pFKD1:GUS*, it is possible that FKD1 and FL1/FL2 either work together later in auxin canalization to cause and maintain PIN polarity within a cell, or that FKD1 is important for the initial establishment of PIN expression domains while FL1 and FL2 maintain these PIN expression domains.

The exact roles of FL1 and FL2 in leaf development are not known, however, like FKD1 it appears that they have some role in the polarization of PIN proteins and vein meeting during leaf development, as the *fkd1/fl2/fl3* mutant has more severe PIN polarity and non-meeting venation defects than the *fkd1* mutant alone (Prabhakaran Mariyamma et al., 2018 in revision; Hou et al., 2010). Given the effects of *fl2* and *fl3* mutation to *fkd1* leaf vein phenotype, it is surprising that *pFL2:GUS* is expressed very late and *pFL3:GUS* is not expressed at all during leaf venation. It is possible that the GUS expression pattern of the reporter constructs in wild type is not representative of the *FL2/FL3* expression in a mutant *fkd1* or *fkd1/fl2/fl3* plant due to functional compensation (Hanada et al., 2010). It is also possible that the expression constructs do not represent the correct transcriptional pattern of the genes. For example, the lost downstream introns in the coding region of the gene may affect expression intensity and location (Rose et al., 2016; Friede et al., 2017).

A final explanation pertaining to *pFL3:GUS* is based on the observation that there is an alternative transcriptional start site in the *FL3* gene that codes for a shorter FL3 isoform (FL3.3). This *FL3.3* transcriptional start site has 5 putative AuxRE element within the first -1000 bp of its TSS (based on analysis by Plant Pan; http://plantpan2.itps.ncku.edu.tw/; Chow et al., 2016), which may indicate strong auxin regulation, and be linked to vascular expression. *pFL3:GUS* was made based on the transcriptional start site for the longest isoform (FL3.1), and thus does not include the 5 AuxRE, which could explain its lack of expression in developing vascular tissue. The *fl3-1* mutant (SALK_013371 from the Arabidopsis Biological Resource Center) used in previous analyses (Prabhakaran Mariyamma et al., 2018 in revision) which knocks out the FL3.1 isoform by *Agrobacterium tumifaciens* Transfer DNA (T-DNA) insertion, is within the FL3.3 promoter (the insertion occurs 70 bp upstream of the transcriptional start site and is between the AuxRE elements and the transcriptional start site). Based on previous analyses of the effects of T-DNA insertion locations on gene expression (O'Malley et al., 2015), the *fl3-1* insertion likely

knocks down the expression of the FL3.3 isoform. Thus, the insertion of the T-DNA in the *fl3-1* mutant likely reduces FL3.3 expression in leaf venation (if it is expressed there) exacerbating the *fkd1* phenotype in the *fkd1/fl3-1* double mutant. To distinguish between these possibilities a first step may be to transform *pFL3:GUS* into *fkd1* to see if the loss of FKD1 protein causes *pFL3:GUS* to be expressed in leaf venation. If *pFL3:GUS* is not expressed in leaf venation in *fkd1* mutants further analysis of the intronic regulation of *FL3* and the FL3.3 isoform will be required to completely understand this gene's regulation during development.

4.2 The Role of *FL*-Genes in Leaf shape and expansion

Of the group I *FL*-genes, only *pFL2:GUS* and *pFL3:GUS* are expressed in leaf epidermal cells during development. Unlike other group I FL-gene family members, *pFL2:GUS* is expressed in the petiole blade junction, and also in proximal leaf margins and within the petiole (Figure 3.4). The *pFL2:GUS* expression pattern suggests that FL2 may be acting in the junction between leaf blade and petiole. The petiole blade junction contains meristematic tissues that provide new cells to both leaves and petioles during development (Ichihashi et al., 2011). Interruption of polar auxin transport at the blade petiole junction by NPA affects leaf size by increasing free IAA levels (Keller et al., 2004), showing that auxin transport in this region is important for leaf expansion. Given the *pFL2:GUS* expression pattern and its proposed function in PIN localization, it is possible that FL2 regulates auxin transport in this region and hence modifies leaf size. In support of this idea, *fl2* mutants have altered leaf area (Prabhakaran Mariyamma et al., 2018 in revision). Like *pFL2:GUS*, *pFL3:GUS* is expressed in the leaf margin, the epidermis of the leaf blade, and in trichomes (Figure 3.5). *pFL3:GUS* expression begins later than the other *FL* genes (~5-6 DAG), indicating that FL3 has unique roles in leaf morphological development. The onset of auxin production by cells within developing leaves (Aloni et al., 2003) corresponds with the distal to proximal progression of the cell cycle arrest front (Andriankaja et al., 2012). Following that

onset, free auxin production occurs in trichomes, stipules, and epidermal cells. The late expression of *pFL3:GUS* in trichomes and epidermal cells may be associated with the production of auxin in those cells. It is possible that pFL3 expression in these regions allows the transport of auxin from sites of synthesis to sink tissues such as the SAM or the ground meristem, which might be important for higher order vein initiation. Another possibility is that with the role of the other group I *FL*-gene family member FKD1 in PIN localization and auxin efflux, and the expression pattern of *pFL2:GUS* and *pFL3:GUS* in the leaf margin and petioles, it is possible that FL2 and FL3 affect SAS responses. As SAS involves changes in leaf size and petiole length through modifications in auxin transport and response (de Wit et al., 2015).

FL-gene promoter:reporter expression in leaves may help to explain the change in epidermal polarity seen in the *fkd1/fl2/*fl3 and the *fkd1/fl1-2/fl2/fl3* mutants (Prabhakaran-Mariyamma, 2015). The *fkd1/fl2/fl3* and the *fkd1/fl1-2/fl2/fl3* mutants often have bract leaf abnormalities where epidermal cells have abnormal polarities, resulting in leaf buckling. This is likely due to abnormal cell division as seen in other similar mutants such as the Maize *tan1* which has epidermal orientation defects attributed to abnormal cell division patterns (Cleary and Smith, 1998), which may be due to polarity defects. Orientation of the plane of cell division in epidermal cells has been shown to be influenced by tensile stress in tissues (Louveaux et al., 2016). It is possible that under normal development, leaf venation provides the major tensile stress in a leaf that regulates the growth axis and coordinates cell division. The reductions in leaf vein meeting and potentially elongation in the *FL*-gene mutants may reduce the overall tensile stress on a leaf allowing cell divisions to be uncoupled from the growth axis resulting in the abnormal epidermal cell polarity.

4.3 The Role of *FL* Genes in Root Development

My analysis of the *FL*-family promoter:reporter fusions suggests that, of the group I *FL*-gene family members, *FKD1*, *FL1*, and *FL2* are expressed in root tissues. In roots, *pFL1:GUS* and *pFL2:GUS* have similar spatial expression that overlaps with *pFKD1:GUS* in the distal meristematic zone (Figure 3.2). It is somewhat surprising that *pFKD1:GUS*, which has previously been shown to be regulated by auxin (Hou et al., 2010), is not strongly expressed in the apical meristematic zone of roots where auxin concentration is highest (Petersson et al., 2009). Both *pFL1:GUS* and *pFL2:GUS* expression occupies the root meristematic region (Figure 3.2) where a higher auxin concentration is predicted. This spatial separation of the FL-gene promoter reporter construct expression may indicate the specialization of these genes in different areas of the root, with FKD1 being more important in the elongation zone of roots while FL1 and FL2 may be important for maintaining and/or modifying the auxin maxima at the RAM.

The expression of *FL*-gene reporter constructs in root tissues is consistent with the root phenotypes seen in plants mutant for several group I *FL*-genes. *pFKD1:GUS*, *pFL1:GUS*, and *pFL2:GUS* are all expressed in the central cylinder of plant roots, likely in the vascular tissue (Figure 3.2). Preliminary root elongation analysis by another lab member (Yu, unpublished results) found that neither the *fkd1* nor *fl1-2* mutants show significant changes in root length or gravitropism compared to the wildtype. However, the *fkd1/fl1-2/fl2/fl3* quadruple mutant and *fkd1/fl1-2* double mutant have significant reductions in root length and gravitropism compared to wild-type, but are not significantly different from each other (Yu, unpublished results). The results indicate that FL2, though expressed in roots, has a minor effect on root development, while FKD1 and FL1 play the major roles. This is interesting, as in roots *pFL1:GUS* has overlapping expression with *pFKD1:GUS* in the distal meristematic zone, up through the elongation and into the differentiation zone of the root. Thus, it is possible that FL1 and FKD1 are able to at least partially compensate for each other. This may result from similar defects to PIN polarization as

seen in the leaves (Prabhakaran Mariyamma et al., 2018 in revision; Hou et al., 2010) preventing auxin transport and re-localization during root development. It would be interesting to look at the size of the zone of elongation and the meristematic zone in mutants more precisely to see if *fkd1* and *fl1* are differentially affecting cell division and elongation within the root.

4.4 *FL* Gene Regulation by Auxin

The expression of *pFKD1:GUS* has previously been shown to be upregulated by treatment with exogenous auxin. The regulation of *pFKD1:GUS* by exogenous auxin may be occurring through its AuxREs (TGTCTC). Support for the idea that *FKD1* was regulated by auxin include reduced transcript in the *axr1-3* mutant as assessed by RT-qPCR, increased expression of *pFKD1:GUS* when grown on 2,4-D plates, and decreased expression of *pFKD1:GUS* in an *mp* (*arf5*) mutant and *axr1-3* mutant (response and synthesis mutants respectively; Hou et al., 2010). However, all of these conditions may cause developmental abnormalities that result in secondary effects that could alter *FKD1* expression. To reduce developmental abnormalities, I treated *pFKD1:GUS* to a much shorter 2,4-D treatment. In agreement with the previous work (Hou et al., 2010), 2,4-D has concentration based effects on *pFKD1:GUS* expression with both 1 μM and 10 uM 2,4-D causing noticeable increases in leaf GUS expression compared to a DMSO control (Figure 3.7). Interestingly, following 10 μM 2,4-D treatment, *pFKD1:GUS* leaf expression is reduced compared to the 1 μM treatment (Figure 3.7). In roots, *pFKD1:GUS* appears to have a different sensitivity to auxin as the 10 μM 2,4-D treatment caused noticeable increases in expression compared to both the DMSO control and the 1 μM 2,4-D treatments. Moreover, in either 2,4-D treated or untreated roots, *pFKD1:GUS* expression does not occur near the root tip (Figure 3.8), which, based on previous studies, has the highest auxin concentration in roots (Petersson et al., 2009). These observations indicate that *pFKD1:GUS* has variable responses to auxin and though upregulated by auxin, may also be regulated by a negative auxin feedback response. The

upregulation of *pFKD1:GUS* by auxin is likely occurring through the AuxRE elements as indicated by the previous *axr1-3*, and *mp* analysis (Hou et al., 2010), and might mean that *FKD1* is up-regulated by ARF5. The region near the root apical meristem where *pFKD1:GUS* is not expressed under untreated conditions contains high auxin concentrations (Petersson et al., 2009) and corresponds to the root expression domain of ARF2 (Rademacher et al., 2011). ARF2 is a repressive ARF protein that may be acting to inhibit *pFKD1:GUS* in this region but not in the distal meristematic or root elongation zone. The expression of ARF2 also increases as leaves age (Gonzalez et al., 2012) and could explain the reduction in *pFKD1:GUS* expression observed in older leaves (Hou et al., 2010). *FKD1* is likely positively regulated by ARF5, when ARF5 is expressed in early leaf development (Wenzel et al., 2007) and is negatively regulated by ARF2, later in leaf development and in tissues where ARF2 is present such as the root meristematic zone where *pFKD1:GUS* is not normally expressed (Gonzalez et al., 2012; Rademacher et al., 2011). In the future, the regulation of *pFKD1:GUS* by repressive ARFs can be tested using a line homozygous for the mutagenized FKD1-A3:GUS construct, or by introducing *pFKD1:GUS* into repressive *ARF* mutants (such as *arf2*).

Comparing the response of *pFKD1:GUS* and *pFL1:GUS* to 2,4-D, indicates that they are divergently regulated by auxin, which may explain some of the spatial and temporal differences in their expression. Like *pFKD1:GUS*, *pFL1:GUS* leaf expression increases in response to 1 μM 2,4-D, although less intensely. Unlike *pFKD1:GUS*, *pFL1:GUS* expression is further increased by 10 μM 2,4-D treatment (Figure 3.7, 3.13). Compared to the DMSO treatment, the 1 μM treatment of 2,4-D increases *pFL1:GUS* expression in the midvein, specifically in the apical half of the leaf. The 10 μM 2,4-D treated *pFL1:GUS* has a more intense expression throughout the midvein, with some additional secondary venation expression occurring (Figure 3.13). Root expression of *pFL1:GUS* increases in response to 1 μM and 10 μM 2,4-D compared to DMSO and all treatments show expression in the meristematic zone. This regulation of *pFL1:GUS* is consistent

with the 3 putative AuxRE elements in its promoter (Figure 3.6) as these elements are likely interacting with ARFs to increase *pFL1:GUS* expression in response to 2,4-D. The different responses of *pFL1:GUS* and *pFKD1:GUS* are interesting, as they indicate that the interaction of AuxREs and increase by 2,4-D expression is not so simple. The classical AuxRE elements (TGTCTC) found by Ulmasov and colleagues (1999) are not the only binding sites for ARF proteins. Recent experiments have shown that there are several other *cis*-regulatory ARF binding motifs (Cherenkov et al., 2018) that may be influencing the regulation of *pFKD1:GUS* and *pFL1:GUS* by auxin. Both MP (ARF5) and ARF2 bind to similar *cis*-regulatory elements, which is why they were proposed to regulate *pFKD1:GUS* expression. *pFL1:GUS* appears to be less responsive to initial increases in 2,4-D than *pFKD1:GUS*. Moreover, *pFL1:GUS* expression in leaves is not suppressed by high auxin concentrations, as 1 μM 2,4-D shows higher expression levels than the DMSO control and 10 μM 2,4-D shows higher expression than the 1 μM treatment (Figure 3.13), unlike the decrease in expression seen in *pFKD1:GUS* leaves at the 10 μM 2,4-D treatment compared to 1 μM 2,4-D (Figure 3.7). These differences in expression could indicate that *pFL1:GUS* is regulated by other factors, which might include different ARF proteins that do not share the same binding site (Cherenkov et al., 2018), or another transcription factor downstream of auxin response. In future analyses, it may be worth further investigating these alternative hexamers and other transcription factors which have not been integrated into the AGRIS program I used for promoter analysis.

4.5 *FL* Gene Regulation by ABA

ABA acts through ABRE elements to upregulate downstream genes. Since both *FKD1* and *FL1* have ABRE-like elements, I expected to see an upregulation of the reporter constructs in response to exogenous ABA. Neither *pFKD1:GUS* or *pFL1:GUS* were upregulated by the addition of exogenous ABA which may be related to the requirement of additional proximal ABRE/ABRE-

like elements for coupling in promoters for upregulation by ABA. Both *pFKD1:GUS* and *pFL1:GUS* contain ABRE elements, however, their placement is unlikely to allow upregulation of gene expression by ABA (Figure 3.6). The *pFKD1:GUS* promoter has only a single ABRE element, a situation which, in other genes, has been shown to require an additional element for the upregulation of gene expression (Narusaka et al., 2003). While *pFL1:GUS* contains several ABRE, these elements are spatially distant from each other, whereas previous examples of ABRE coupling required that sites be 70-100 bp (Narusaka et al., 2003) or 5 bp (Mikkelsen and Thomashow, 2009) from each other. Since another ABRE/ABRE-like element isn't present in either of the *pFKD1:GUS* or *pFL1:GUS* promoters close enough to couple it makes sense that these genes are not up-regulated by ABA treatment alone.

The addition of exogenous ABA down regulated both *pFKD1:GUS* (Figure 3.9, 3.10) and *pFL1:GUS* expression (Figure 3.15, 3.16). The repression of expression by ABA is less well characterized than its activation as it does not involve a conserved ABA repressive *cis*-regulatory motif (ABRE) and likely acts through negative interactions with growth stimulating hormones such as auxin, gibberellic acid, and brassinosteroids. ABA and auxin signaling interact at several points in root and leaf development. Where ABA repression has been characterized, it involves hormonal cross-talk with other pathways such as auxin via upregulation of ARF2 or repression of TIR1/AFB2 proteins by MIR393 expression (Wang et al., 2011a; Chen et al., 2011). The general repression of growth by ABA may be due to crosstalk with the gibberellins or brassinosteroid pathways that have been shown to antagonize and modify ABA responses (Ha et al., 2016; Hu and Yu, 2014; Divi et al., 2010; Colebrook et al., 2014). Brassinosteroids and gibberellins both play important roles in promoting plant growth, and their reduction could be negatively affecting the expression of *pFKD1:GUS* and *pFL1:GUS* in response to ABA. In future studies, it may be beneficial to expand my hormone studies to include the application of exogenous gibberellic acid and brassinosteroids inhibitors to narrow down how ABA may be repressing these genes.

4.6 *FL* Gene Regulation by Mannitol and NaCl

4.6.1 Mannitol and NaCl regulation in leaves

Although the expression of *pFKD1:GUS* and *pFL1:GUS* are similar in response to ABA, the responses of the two reporter constructs differ when treated with osmotic and salt stress. In leaves, *pFL1:GUS* expression is largely reduced at increasing concentrations of mannitol and NaCl, with the NaCl treatments causing more substantial decreases in *pFL1:GUS* expression (Figure 3.17). In contrast, *pFKD1:GUS* shows a dose dependent response with low concentrations of mannitol (150 mM) and NaCl (100 mM) reducing reporter expression, while at higher treatments (mannitol; 300 mM and NaCl 150 mM) the levels of *pFKD1:GUS* expression are similar to the control leaves (Figure 3.11). The identified putative promoter elements of *FKD1* and *FL1* may help to explain why this is occurring. In the *pFL1:GUS* promoter construct, there are no DRE elements and the ABRE-like elements are likely too widely spaced to couple with each other (Figure 3.6). In contrast, the *pFKD1:GUS* promoter has a single ABRE-like element which is near a DRE-like element (Figure 3.6). If coupling of these elements occurs, it could explain the increase in expression at high concentrations of NaCl (150 mM) and Mannitol (300 mM) in roots and the similarity to untreated control expression levels in leaves (Figure 3.11, 3.12). The decrease in *pFKD1:GUS* expression in leaves in response to low concentrations of Mannitol and NaCl may be from an initial ABA or stress related response which likely occurs independently of the ABRE-like elements. Negative regulation of *pFKD1:GUS* occurring indirectly by ABA is consistent with the reduced p*FKD1:GUS* expression seen following treatment with ABA (Figure 3.9, 3.10). Furthermore, DREB2A expression is itself induced by the expression of ABA and DREB2A protein is induced only after 7.5-10 hours of severe dehydration stress (Kim et al., 2011; Morimoto et al., 2013). I suggest that the higher concentrations of NaCl and Mannitol are able to induce immediate ABA synthesis and downstream DREB2A expression similar to the

extreme dehydration stress imposed on Arabidopsis in the study by Morimoto and colleagues (2013). The lower concentrations of mannitol and NaCl are too low to trigger sufficient ABA synthesis and resulting DREB2A expression. This lack of induction of DREB2A would explain why *pFKD1:GUS* expression decreases in the lower stress treatments, but is similar to the DMSO control at higher treatments. Though most expression analysis has focused in the -1 to -1000 bp from the TSS, the ABRE *cis*-regulatory region between -2664 and -2018 bp from the TSS was critical for *AtNCED3* response to ABA (Yang and Tan 2014). This *AtNCED3* ABRE response requires ABRE elements more distal than the *pFKD1:GUS* ABRE element supporting the possibility that such a distal element is regulating *pFKD1:GUS* response to these stresses.

4.6.2. Mannitol and NaCl Regulation in Roots

In roots, *pFL1:GUS* and *pFKD1:GUS* expression regulation by mannitol and NaCl diverge from each other as well. At high concentrations of mannitol (300 mM) and NaCl (150 mM) *pFKD1:GUS* root expression is increased over the control and the lower mannitol (150 mM) and NaCl (150 mM) concentrations. The *pFL1:GUS* root expression is relatively unaffected by mannitol treatment, but is sharply reduced at higher NaCl (150 mM) concentrations. This is interesting as, though osmotic stress and salt stress tend to have similar effects on root morphology, there are some subtle differences between the two. The most obvious difference is that drought stress does not affect root primary elongation, but limits lateral root formation (Deak and Malamy, 2005; Seo and Park, 2009). In contrast, NaCl causes a partial osmotic stress, and results in increased lateral root initiation and emergence and, through the SOS pathway, reduced primary root growth (Zhao et al., 2011). Increased lateral root initiation and elongation both occur due to increased auxin synthesis and transport from the shoot to the RAM and then into root epidermal cells. A tempting idea, based on the change in expression patterns of the *pFKD1:GUS* and *pFL1:GUS* constructs in response to salt and osmotic stress, is that FKD1 is involved in the

transport of auxin from the shoot to the distal meristematic zone whereas FL1 is involved in influencing auxin transport to maintain the RAM auxin maxima and maintain primary root growth under drought. The change in *pFKD1:GUS* expression is likely regulated by the previously mentioned ABRE-like and DRE-like elements in its promoter, and altered FKD1 expression may cause changes in auxin transport during stress to influence root morphology. Under salt stress conditions, FL1 expression may then decrease the ability to maintain an auxin maxima in the root apical meristem, favouring the transport of auxin to root epidermal cells resulting in more lateral roots. This idea could be tested by treating *fkd1* and *fl1* with mannitol and NaCl to observe if the root morphology such as root length and lateral root number responds differently. The expected result based on this hypothesis would be that the *fl1* mutant would have similar numbers of lateral roots and primary root elongation under osmotic stress as salt stress. In *fkd1*, one might expect that the reductions in polar PIN1 localization in osmotically stressed roots (Rowe et al., 2016) would be exacerbated by the *fkd1* mutation, which should further reduce both root length and lateral root formation.

Some additional possibilities for future analysis of the roles of the *FL*-gene family in environmental stress response include analysis of the other family members and further elaboration of the regulatory *cis*-elements. Zhao and colleagues (2011), during their analysis of auxin synthesis in response to NaCl, showed that NaCl stress can increase *DR5:GUS* expression in the apical margins of cotyledons. The expression of *DR5:GUS* occurs in a similar location to *pFL3:GUS* in cotyledons (Figure 3.1). It is possible that, in response to NaCl stress, increases of auxin synthesis or response in this region may regulate *pFL3:GUS* expression, especially with *pFKD1:GUS* and *pFL1:GUS* responding to drought and osmotic stress. I have also developed a set of DRE-like and ABRE-like *pFKD1:GUS* mutants to address the question of whether the DRE and ABRE regions are important in osmotic stress response, however, I was unable to develop homozygous lines. Further evaluation of these mutagenized lines would provide strong evidence

for either the regulation of *FKD1* by a relatively distal promoter combination or the possibility of another unidentified form of regulation, both of which would be interesting results.

4.7 Conclusions

The FL-gene reporter constructs are expressed at critical stages of plant development and correspond well to the phenotypes observed by mutant analysis providing support to previous hypotheses for the roles of the group I *FL*-genes. Overlapping expression patterns of *pFKD1:GUS*, *pFL1:GUS*, and *pFL2:GUS* support previous phenotypic analyses (Prabhakaran Mariyamma et al., 2018 in revision) that implicate the *FL*-genes in developmental processes related to PIN polarization and auxin transport during root and leaf vascular development. The regulation of *pFKD1:GUS* and *pFL1:GUS* by auxin supports the hypothesis that alterations in auxin signalling and transport such as auxin canalization may be regulating these genes, and modifying their expression during vascular formation to cooperatively work to canalize PIN proteins. This thesis proposes that the *FL*-genes may be regulated in a gene specific manner to alter plant development during osmotic and NaCl stresses, however, this will have to be further tested by morphological studies. Though there is a lot of similarity among the group I *FL*-genes, *FKD1* is the most divergent member with the most prominent phenotype. Differences in gene expression and regulation among the members shown in this thesis and in the protein products intracellular localization (Prabhakaran Mariyamma et al., 2018 in revision) may indicate that the gene family has other unique and undiscovered roles, perhaps during stress responses, or in the localization of other proteins.

References

Abley, K., Sauret-Güeto, S., Marée, A.F.M., and Coen, E. (2016). Formation of Polarity Convergences Underlying Shoot Outgrowths. Elife **5**: 1–43.

Adamowski, M. and Friml, J. (2015). PIN-Dependent Auxin Transport: Action, Regulation, and Evolution. Plant Cell **27**: 20–32.

Aloni, R., Schwalm, K., Langhans, M., and Ullrich, C.I. (2003). Gradual Shifts in Sites of Free-Auxin Production During Leaf-Primordium Development and Their Role in Vascular Differentiation and Leaf Morphogenesis in Arabidopsis. Planta **216**: 841–853.

Andriankaja, M., Dhondt, S., DeBodt, S., Vanhaeren, H., Coppens, F., DeMilde, L., Mühlenbock, P., Skirycz, A., Gonzalez, N., Beemster, G.T.S., and Inzé, D. (2012). Exit From Proliferation During Leaf Development in Arabidopsis thaliana: A Not-So-Gradual Process. Dev. Cell **22**: 64–78.

Band, L.R. et al. (2012). Root Gravitropism Is Regulated by a Transient Lateral Auxin Gradient Controlled by a Tipping-Point Mechanism. Proc. Natl. Acad. Sci. **109**: 4668–4673.

Basu, S., Ramegowda, V., Kumar, A., and Pereira, A. (2016). Plant Adaptation to Drought Stress. F1000Research **5**: 1–10.

Bayer, E.M., Smith, R.S., Mandel, T., Nakayama, N., Sauer, M., Prusinkiewicz, P., and Kuhlemeier, C. (2009). Integration of Transport-Based Models For Phyllotaxis and Midvein Formation. Genes Dev. **23**: 373–384.

Benjamins, R., Quint, A., Weijers, D., Hooykaas, P., and Offringa, R. (2001). The PINOID Protein Kinase Regulates Organ Development in Arabidopsis by Enhancing Polar Auxin Transport. Development **128**: 4057–4067.

Bi, H., Kovalchuk, N., Langridge, P., Tricker, P.J., Lopato, S., and Borisjuk, N. (2017). The Impact of Drought on Wheat Leaf Cuticle Properties. BMC Plant Biol. **17**: 1–13.

Bilsborough, G.D., Runions, A., Barkoulas, M., Jenkins, H.W., Hasson, A., Galinha, C., Laufs, P., Hay, A., Prusinkiewicz, P., and Tsiantis, M. (2011). Model For The Regulation of Arabidopsis thaliana Leaf Margin Development. Proc. Natl. Acad. Sci. **108**: 3424–3429.

Blein, T., Pulido, A., Vialette-Guiraud, A., Nikovics, K., Morin, H., Hay, A., Johansen, I.E., Tsiantis, M., and Laufs, P. (2008). A Conserved Molecular Framework for Compound Leaf Development. Science (80-.). **322**: 1835–1839.

Blilou, I., Xu, J., Wildwater, M., Willemsen, V., Paponov, I., Friml, J., Heidstra, R., Aida, M., Palme, K., and Scheres, B. (2005). The PIN Auxin Efflux Facilitator Network Controls Growth And Patterning in Arabidopsis Roots. Nature **433**: 39–44.

de Boer, H.J., Drake, P.L., Wendt, E., Price, C.A., Schulze, E.-D., Turner, N.C., Nicolle, D., and Veneklaas, E.J. (2016). Apparent Overinvestment in Leaf Venation Relaxes Leaf Morphological Constraints on Photosynthesis in Arid Habitats. Plant Physiol. **172**: 2286–2299.

De Boer, H.J., Eppinga, M.B., Wassen, M.J., and Dekker, S.C. (2012). A Critical Transition in Leaf Evolution Facilitated The Cretaceous Angiosperm Revolution. Nat. Commun. **3**: 1–11.

Busk, P.K. and Pagès, M. (1998). Regulation of Abscisic Acid-Induced Transcription. Plant Mol. Biol. **37**: 425–435.

Cajero Sánchez, W., García-Ponce, B., Sánchez, M. de la P., Álvarez-Buylla, E.R., and Garay-Arroyo, A. (2017). Identifying the Transition to The Maturation Zone in Three Ecotypes Of Arabidopsis thaliana Roots. Commun. Integr. Biol. **0889**: e1395993.

Chan, K.X., Mabbitt, P.D., Phua, S.Y., Mueller, J.W., Nisar, N., Gigolashvili, T., Stroeher, E., Grassl, J., Arlt, W., Estavillo, G.M., Jackson, C.J., and Pogson, B.J. (2016). Sensing and Signaling of Oxidative Stress in Chloroplasts by Inactivation of the SAL1 Phosphoadenosine Phosphatase. Proc. Natl. Acad. Sci. **113**: E4567–E4576.

Chen, W. et al. (2002). Expression Profile Matrix of Arabidopsis Transcription Factor Genes Suggests Their Putative Functions in Response to Environmental Stresses. Plant Cell **14**: 559–574.

Chen, Z.H., Bao, M.L., Sun, Y.Z., Yang, Y.J., Xu, X.H., Wang, J.H., Han, N., Bian, H.W., and Zhu, M.Y. (2011). Regulation of Auxin Response by miR393-Targeted Transport Inhibitor Response Protein 1 is Involved in Normal Development in Arabidopsis. Plant Mol. Biol. **77**: 619–629.

Cheng, M.-C., Liao, P.-M., Kuo, W.-W., and Lin, T.-P. (2013). The Arabidopsis ETHYLENE RESPONSE FACTOR1 Regulates Abiotic Stress-Responsive Gene Expression by Binding to Different cis-Acting Elements in Response to Different Stress Signals. Plant Physiol. **162**: 1566–1582.

Cheng, W.H., Chiang, M.H., Hwang, S.G., and Lin, P.C. (2009). Antagonism Between Abscisic Acid and Ethylene in Arabidopsis Acts in Parallel With the Reciprocal Regulation Of Their Metabolism And Signaling Pathways. Plant Mol. Biol. **71**: 61–80.

Cheng, Y., Dai, X., and Zhao, Y. (2006). Auxin Biosynthesis by the YUCCA Flavin Monooxygenases Controls the Formation of Floral Organs and Vascular Tissues in Arabidopsis. Genes Dev. **20**: 1790–1799.

Cherenkov, P., Novikova, D., Omelyanchuk, N., Levitsky, V., Grosse, I., Weijers, D., and Mironova, V. (2018). Diversity of cis-Regulatory Elements Associated with Auxin Response in Arabidopsis thaliana. J. Exp. Bot. **69**: 329–339.

Choi, H.-I., Hong, J.-H., Ha, J.-O., Kang, J.-Y., and Kim, S.Y. (2000). ABFs, a Family of ABA Responsive Element Binding Factors. J. Biol. Chem. **275**: 1723–1730.

Chow, C.N., Zheng, H.Q., Wu, N.Y., Chien, C.H., Huang, H. Da, Lee, T.Y., Chiang-Hsieh, Y.F., Hou, P.F., Yang, T.Y., and Chang, W.C. (2016). PlantPAN 2.0: An Update of Plant Promoter Analysis Navigator for Reconstructing Transcriptional Regulatory Networks in Plants. Nucleic Acids Res. **44**: D1154–D1164.

Clauw, P. et al. (2016). Leaf Growth Response to Mild Drought: Natural Variation in Arabidopsis Sheds Light on Trait Architecture. Plant Cell **28**: 2417–2434.

Cleary, A.L. and Smith, L.G. (1998). The Tangled1 Gene is Required for Spatial Control of Cytoskeletal Arrays Associated with Cell Division During Maize Leaf Development. Plant Cell **10**: 1875–1888.

Colebrook, E.H., Thomas, S.G., Phillips, A.L., and Hedden, P. (2014). The Role of Gibberellin Signalling in Plant Responses to Abiotic Stress. J. Exp. Biol. **217**: 67–75.

Cosgrove, D.J. (1993). How Do Plant Cell Walls Extend? Plant Physiol. **102**: 1–6.

Davuluri, R. V., Sun, H., Palaniswamy, S.K., Matthews, N., Molina, C., Kurtz, M., and

Grotewold, E. (2003). AGRIS: Arabidopsis Gene Regulatory Information Server, an Information Resource of Arabidopsis cis-Regulatory Elements and Transcription Factors. BMC Bioinformatics **4**: 1–11.

Deak, K.I. and Malamy, J. (2005). Osmotic Regulation of Root System Architecture. Plant J. **43**: 17–28.

Deb, Y., Marti, D., Frenz, M., Kuhlemeier, C., and Reinhardt, D. (2015). Phyllotaxis Involves Auxin Drainage Through Leaf Primordia. Development **142**: 1992–2001.

Dharmasiri, N., Dharmasiri, S., Weijers, D., Lechner, E., Yamada, M., Hobbie, L., Ehrismann, J.S., Jürgens, G., and Estelle, M. (2005). Plant Development is Regulated by a Family of Auxin Receptor F Box Proteins. Dev. Cell **9**: 109–119.

Divi, U.K., Rahman, T., and Krishna, P. (2010). Brassinosteroid-Mediated Stress Tolerance in Arabidopsis Shows Interactions with Abscisic Acid, Ethylene and Salicylic Acid Pathways. BMC Plant Biol. **10**: 151.

Doerner, P., Jorrgensen, J.-E., R., Y., Steppuhn, J., and Lamb., C.L.B.-P.B.S.R. 4860 (1996). Control of Root Growth and Development by Cyclin Expression. Nature **380**: 520–523.

Doyle, S.M., Haeger, A., Vain, T., Rigal, A., Viotti, C., Łangowska, M., Ma, Q., Friml, J., Raikhel, N. V., Hicks, G.R., and Robert, S. (2015). An Early Secretory Pathway Mediated by GNOM-LIKE 1 and GNOM is Essential for Basal Polarity Establishment in Arabidopsis thaliana. Proc. Natl. Acad. Sci. **112**: E806–E815.

Du, W., Lin, H., Chen, S., Wu, Y., Zhang, J., Fuglsang, A.T., Palmgren, M.G., Wu, W., and Guo, Y. (2011). Phosphorylation of SOS3-Like Calcium-Binding Proteins by Their Interacting SOS2-Like Protein Kinases Is a Common Regulatory Mechanism in Arabidopsis. Plant Physiol. **156**: 2235–2243.

Du, Y. and Scheres, B. (2018). Lateral Root Formation and the Multiple Roles of Auxin. J. Exp. Bot. **69**: 155–167.

Feild, T.S., Brodribb, T.J., Iglesias, A., Chatelet, D.S., Baresch, A., Upchurch, G.R., Gomez, B., Mohr, B.A.R., Coiffard, C., Kvacek, J., and Jaramillo, C. (2011). Fossil Evidence for Cretaceous Escalation in Angiosperm Leaf Vein Evolution. Proc. Natl. Acad. Sci. **108**: 8363–8366.

Ferreira, P., Hemerly, a, de Almeida Engler, J., Bergounioux, C., Burssens, S., Van Montagu, M., Engler, G., and Inzé, D. (1994). Three Discrete Classes of Arabidopsis Cyclins are Expressed During Different Intervals of the Cell Cycle. Proc. Natl. Acad. Sci. U. S. A. **91**: 11313–11317.

Finkelstein, R. (2013). Abscisic Acid Synthesis and Response. Arab. B. **11**: e0166.

Fiorin, L., Brodribb, T.J., and Anfodillo, T. (2016). Transport Efficiency Through Uniformity: Organization of Veins and Stomata in Angiosperm Leaves. New Phytol. **209**: 216–227.

Friede, A., Zhang, B., Herberth, S., Pesch, M., Schrader, A., and Hülskamp, M. (2017). The Second Intron Is Essential for the Transcriptional Control of the Arabidopsis thaliana GLABRA3 Gene in Leaves. Front. Plant Sci. **8**: 1382.

Friml, J., Vieten, A., Sauer, M., Weijers, D., Schwarz, H., Hamann, T., Offringa, R., and Jürgens, G. (2003). Efflux-Dependent Auxin Gradients Establish the Apical-Basal Axis of Arabidopsis. Nature **426**: 147–153.

Geldner, N., Anders, N., Wolters, H., Keicher, J., Kornberger, W., Muller, P., Delbarre, A., Ueda, T., Nakano, A., and Jürgens, G. (2003). The Arabidopsis GNOM ARF-GEF Mediates Endosomal Recycling, Auxin Transport, and Auxin-Dependent Plant Growth. Cell **112**: 219–230.

Gonzalez, N., Vanhaeren, H., and Inzé, D. (2012). Leaf Size Control: Complex Coordination of Cell Division and Expansion. Trends Plant Sci. **17**: 332–340.

Gorai, M., Laajili, W., Santiago, L.S., and Neffati, M. (2015). Rapid Recovery of Photosynthesis and Water Relations Following Soil Drying and Re-Watering is Related to the Adaptation of Desert Shrub Ephedra Alata Subsp. alenda (ephedraceae) to Arid Environments. Environ. Exp. Bot. **109**: 113–121.

Guan, Q., Wu, J., Yue, X., Zhang, Y., and Zhu, J. (2013). A Nuclear Calcium-Sensing Pathway Is Critical for Gene Regulation and Salt Stress Tolerance in Arabidopsis. PLoS Genet. **9**: e1003755.

Guenot, B., Bayer, E., Kierzkowski, D., Smith, R.S., Mandel, T., Zadnikova, P., Benkova, E., and Kuhlemeier, C. (2012). PIN1-Independent Leaf Initiation in Arabidopsis. Plant Physiol. **159**: 1501–1510.

Guilfoyle, T.J. and Hagen, G. (2007). Auxin Response Factors. Curr. Opin. Plant Biol. **10**: 453–460.

Guiltinan, M.J., Marcotte Jr., W.R., and Quatrano, R.S. (1990). A Plant Leucine Zipper Protein that Recognizes an Abscisic Acid Response Element. Science. **250**: 267–271.

Guo, L., Yang, H., Zhang, X., and Yang, S. (2013). Lipid Transfer Protein 3 as a Target of Myb96 Mediates Freezing and Drought Stress in Arabidopsis. J. Exp. Bot. **64**: 1755–1767.

Ha, Y., Shang, Y., and Nam, K.H. (2016). Brassinosteroids Modulate ABA-Induced Stomatal Closure in Arabidopsis. J. Exp. Bot. **67**: 6297–6308.

Habets, M.E.J. and Offringa, R. (2014). PIN-driven Polar Auxin Transport in Plant Developmental Plasticity: A Key Target For Environmental and Endogenous Signals. New Phytol. **203**: 362–377.

Hanada, K., Kuromori, T., Myouga, F., Toyoda, T., Li, W.H., and Shinozaki, K. (2010). Evolutionary Persistence of Functional Compensation by Duplicate Genes in Arabidopsis. Genome Biol. Evol. **1**: 409–414.

Harb, A., Krishnan, A., Ambavaram, M.M.R., and Pereira, A. (2010). Molecular and Physiological Analysis of Drought Stress in Arabidopsis Reveals Early Responses Leading to Acclimation in Plant Growth. Plant Physiol. **154**: 1254–1271.

Heisler, M.G., Ohno, C., Das, P., Sieber, P., Reddy, G. V., Long, J.A., and Meyerowitz, E.M. (2005). Patterns of Auxin Transport and Gene Expression During Primordium Development Revealed by Live Imaging of the Arabidopsis Inflorescence Meristem. Curr. Biol. **15**: 1899–1911.

Hou, H., Erickson, J., Meservy, J., and Schultz, E.A. (2010). FORKED1 Encodes a PH Domain Protein that is Required for PIN1 Localization in Developing Leaf Veins. Plant J. **63**: 960–973.

Hu, Y. and Yu, D. (2014). BRASSINOSTEROID INSENSITIVE2 Interacts with ABSCISIC ACID INSENSITIVE5 to Mediate the Antagonism of Brassinosteroids to Abscisic Acid

during Seed Germination in *Arabidopsis*. Plant Cell Online **26**: 4394–4408.

Huang, F., Luo, J., Ning, T., Cao, W., Jin, X., Zhao, H., Wang, Y., and Han, S. (2017). Cytosolic and Nucleosolic Calcium Signaling in Response to Osmotic and Salt Stresses Are Independent of Each Other in Roots of Arabidopsis Seedlings. Front. Plant Sci. **8**: 1–13.

Ichihashi, Y., Kawade, K., Usami, T., Horiguchi, G., Takahashi, T., and Tsukaya, H. (2011). Key Proliferative Activity in the Junction Between the Leaf Blade and Leaf Petiole of Arabidopsis. Plant Physiol. **157**: 1151–1162.

Iwakawa, H., Iwasaki, M., Kojima, S., Ueno, Y., Soma, T., Tanaka, H., Semiarti, E., Machida, Y., and Machida, C. (2007). Expression of the ASYMMETRIC LEAVES2 Gene in the Adaxial Domain of Arabidopsis Leaves Represses Cell Proliferation In This Domain And Is Critical For The Development Of Properly Expanded Leaves. Plant J. **51**: 173–184.

Izhaki, A. and Bowman, J.L. (2007). KANADI and Class III HD-Zip Gene Families Regulate Embryo Patterning and Modulate Auxin Flow during Embryogenesis in Arabidopsis. Plant Cell Online **19**: 495–508.

Ji, H., Pardo, J.M., Batelli, G., Van Oosten, M.J., Bressan, R.A., and Li, X. (2013). The Salt Overly Sensitive (SOS) Pathway: Established and Emerging Roles. Mol. Plant **6**: 275–286.

Jones, A.M., Danielson, J.Å.H., Manojkumar, S.N., Lanquar, V., Grossmann, G., and Frommer, W.B. (2014). Abscisic Acid Dynamics in Roots Detected with Genetically Encoded FRET Sensors. Elife **2014**: 1–30.

Kasuga, M., Liu, Q., Miura, S., Yamaguchi-Shinozaki, K., and Shinozaki, K. (1999). Improving Plant Drought, Salt, and Freezing Tolerance by Gene Transfer of a Single Stress-Inducible Transcription Factor. Nat. Biotechnol. **17**: 287–291.

Kawamura, E., Horiguchi, G., and Tsukaya, H. (2010). Mechanisms of Leaf Tooth Formation in Arabidopsis. Plant J. **62**: 429–441.

Kazachkova, Y., Batushansky, A., Cisneros, A., Tel-Zur, N., Fait, A., and Barak, S. (2013). Growth Platform-Dependent and -Independent Phenotypic and Metabolic Responses of Arabidopsis and Its Halophytic Relative, Eutrema salsugineum, to Salt Stress. Plant Physiol. **162**: 1583–1598.

Kazan, K. and Lyons, R. (2016). The Link Between Flowering Time and Stress Tolerance. J. Exp. Bot. **67**: 47–60.

Keller, C.P., Stahlberg, R., Barkawi, L.S., and Cohen, J.D. (2004). Long-Term Inhibition by Auxin of Leaf Blade Expansion in Bean and Arabidopsis. Plant Physiol. **134**: 1217–1226.

Kim, J.S., Mizoi, J., Yoshida, T., Fujita, Y., Nakajima, J., Ohori, T., Todaka, D., Nakashima, K., Hirayama, T., Shinozaki, K., and Yamaguchi-Shinozaki, K. (2011). An ABRE Promoter Sequence is Involved in Osmotic stress-Responsive Expression of the DREB2A Gene, which Encodes a Transcription Factor Regulating Drought-Inducible Genes in Arabidopsis. Plant Cell Physiol. **52**: 2136–2146.

Kleine-Vehn, J. et al. (2011). Recycling, Clustering, and Endocytosis Jointly Maintain PIN Auxin Carrier Polarity at the Plasma Membrane. Mol. Syst. Biol. **7**: 1–13.

Koevoets, I.T., Venema, J.H., Elzenga, J.T.M., and Testerink, C. (2016). Roots Withstanding their Environment: Exploiting Root System Architecture Responses to Abiotic Stress to Improve Crop Tolerance. Front. Plant Sci. **07**: 1–19.

Koizumi, K., Naramoto, S., Sawa, S., Yahara, N., Ueda, T., Nakano, A., Sugiyama, M., Fukuda, H., and 1Department (2005). VAN3 ARF-GAP-Mediated Vesicle Transport is Involved in Leaf Vascular Network Formation. Development **132**: 1699–1711.

Kondo, Y., Tamaki, T., and Fukuda, H. (2014). Regulation of Xylem Cell Fate. Front. Plant Sci. **5**: 1–6.

Kosma, D.K., Bourdenx, B., Bernard, A., Parsons, E.P., Lu, S., Joubes, J., and Jenks, M.A. (2009). The Impact of Water Deficiency on Leaf Cuticle Lipids of Arabidopsis. Plant Physiol. **151**: 1918–1929.

Kozuka, T., Kobayashi, J., Horiguchi, G., Demura, T., Sakakibara, H., Tsukaya, H., and Nagatani, A. (2010). Involvement of Auxin and Brassinosteroid in the Regulation of Petiole Elongation under the Shade. Plant Physiol. **153**: 1608–1618.

Krasensky, J. and Jonak, C. (2012). Drought, Salt, and Temperature Stress-Induced Metabolic Rearrangements and Regulatory Networks. J. Exp. Bot. **63**: 1593–1608.

Langowski, L., Wabnik, K., Li, H., Vanneste, S., Naramoto, S., Tanaka, H., and Friml, J. (2016). Cellular Mechanisms for Cargo Delivery and Polarity Maintenance at Different Polar Domains in Plant Cells. Cell Discov. **2**: 16081.

Laskowski, M., Grieneisen, V.A., Hofhuis, H., Ten Hove, C.A., Hogeweg, P., Marée, A.F.M., and Scheres, B. (2008). Root System Architecture from Coupling Cell Shape to Auxin Transport. PLoS Biol. **6**: 2721–2735.

Lata, C. and Prasad, M. (2011). Role of DREBs in Regulation of Abiotic Stress Responses in Plants. J. Exp. Bot. **62**: 4731–4748.

Lee, S.W., Feugier, F.G., and Morishita, Y. (2014). Canalization-Based Vein Formation in a Growing Leaf. J. Theor. Biol. **353**: 104–120.

Leitz, G., Kang, B.-H., Schoenwaelder, M.E.A., and Staehelin, L.A. (2009). Statolith Sedimentation Kinetics and Force Transduction to the Cortical Endoplasmic Reticulum in Gravity-Sensing Arabidopsis Columella Cells. Plant Cell **21**: 843–60.

Lezin, G., Kosaka, Y., Yost, H.J., Kuehn, M.R., and Brunelli, L. (2011). A One-Step Miniprep for the Isolation of Plasmid DNA and Lambda Phage Particles. PLoS One **6**: e23457.

Li, L. et al. (2012). Linking Photoreceptor Excitation to Changes in Plant Architecture Linking Photoreceptor Excitation to Changes in Plant Architecture. Genes Dev. **26**: 785–790.

Li, X., Chen, L., Forde, B.G., and Davies, W.J. (2017). The Biphasic Root Growth Response to Abscisic Acid in Arabidopsis Involves Interaction with Ethylene and Auxin Signalling Pathways. Front. Plant Sci. **8**: 1–12.

Lim, P.O., Lee, I.C., Kim, J., Kim, H.J., Ryu, J.S., Woo, H.R., and Nam, H.G. (2010). AUXIN RESPONSE FACTOR 2 (ARF2) Plays a Major Role in Regulating Auxin-Mediated Leaf Longevity. J. Exp. Bot. **61**: 1419–1430.

Lima, J.E., Kojima, S., Takahashi, H., and von Wiren, N. (2010). Ammonium Triggers Lateral Root Branching in Arabidopsis in an AMMONIUM TRANSPORTER1;3-Dependent Manner. Plant Cell Online **22**: 3621–3633.

Lin, W., Shuai, B., and Springer, P.S. (2003). The Arabidopsis LATERAL ORGAN BOUNDARIES –Domain Gene ASYMMETRIC LEAVES2 Functions in the Repression of

KNOX Gene Expression and in Adaxial-Abaxial Patterning. Plant Cell **15**: 2241–2252.

Liu, Q., Kasuga, M., Sakuma, Y., Abe, H., Miura, S., Yamaguchi-Shinozaki, K., and Shinozaki, K. (1998). Two Transcription Factors, DREB1 and DREB2, with an EREBP/AP2 DNA Binding Domain Separate Two Cellular Signal Transduction Pathways in Drought- and Low-Temperature-Responsive Gene Expression, Respectively, in Arabidopsis. Plant Cell **10**: 1391–1406.

Louveaux, M., Julien, J.-D., Mirabet, V., Boudaoud, A., and Hamant, O. (2016). Cell Division Plane Orientation Based on Tensile Stress in Arabidopsis thaliana. Proc. Natl. Acad. Sci. **113**: E4294–E4303.

Mähönen, A.P., Tusscher, K., Siligato, R., and Smetana, O. (2014). PLETHORA Gradient Formation Mechanism Separates Auxin Responses. Nature **515**: 125–129.

Di Mambro, R. et al. (2017). Auxin Minimum Triggers the Developmental Switch from Cell Division to Cell Differentiation in the Arabidopsis Root. Proc. Natl. Acad. Sci. **114**: E7641–E7649.

Manzi, M., Lado, J., Rodrigo, M.J., Zacariás, L., Arbona, V., and Gómez-Cadenas, A. (2015). Root ABA Accumulation in Long-Term Water-Stressed Plants is Sustained by Hormone Transport from Aerial Organs. Plant Cell Physiol. **56**: 2457–2466.

Masson, P.H., Tasaka, M., Morita, M.T., Guan, C., Chen, R., and Boonsirichai, K. (2002). Arabidopsis thaliana: A Model for the Study of Root and Shoot Gravitropism. Arab. B. **35**: 1.

McAdam, S.A.M., Brodribb, T.J., and Ross, J.J. (2016). Shoot-Derived Abscisic Acid Promotes Root Growth. Plant. Cell Environ. **39**: 652–659.

Merelo, P., Ram, H., Pia Caggiano, M., Ohno, C., Ott, F., Straub, D., Graeff, M., Cho, S.K., Yang, S.W., Wenkel, S., and Heisler, M.G. (2016). Regulation of *MIR165/166* by Class II and Class III Homeodomain Leucine Zipper Proteins Establishes Leaf Polarity. Proc. Natl. Acad. Sci. **113**: 11973–11978.

Michniewicz, M. et al. (2007). Antagonistic Regulation of PIN Phosphorylation by PP2A and PINOID Directs Auxin Flux. Cell **130**: 1044–1056.

Mikkelsen, M.D. and Thomashow, M.F. (2009). A Role for Circadian Evening Elements in Cold-Regulated Gene Expression in Arabidopsis. Plant J. **60**: 328–339.

Moreno-Risueno, M.A., Van Norman, J.M., Moreno, A., Zhang, J., Ahnert, S.E., and Benfey, P.N. (2010). Oscillating Gene Expression Determines Competence for Periodic Arabidopsis Root Branching. Science (80-.). **329**: 1306–1311.

Morimoto, K., Mizoi, J., Qin, F., Kim, J.S., Sato, H., Osakabe, Y., Shinozaki, K., and Yamaguchi-Shinozaki, K. (2013). Stabilization of Arabidopsis DREB2A is Required but not Sufficient for the Induction of Target Genes Under Conditions of Stress. PLoS One **8**: e80457.

Mundy, J., Yamaguchi-Shinozaki, K., and Chua, N.H. (1990). Nuclear Proteins Bind Conserved Elements in the Abscisic Acid-Responsive Promoter of a Rice Rab Gene. Proc. Natl. Acad. Sci. U. S. A. **87**: 1406–1410.

Nakashima, K., Shinwari1, Z.K., Sakuma, Y., Seki, M., Miura, S., Shinozaki, K., and Yamaguchi-Shinozaki, K. (2000). Organization and Expression of Two Arabidopsis

DREB2 Genes Encoding DRE-Binding Proteins Involved in Dehydration- and High-Salinity-Responsive Gene Expression. Plant Mol. Biol. **42**: 657–665.

Naramoto, S., Sawa, S., Koizumi, K., Uemura, T., Ueda, T., Friml, J., Nakano, A., and Fukuda, H. (2009). Phosphoinositide-Dependent Regulation of VAN3 ARF-GAP Localization and Activity Essential for Vascular Tissue Continuity in Plants. Development **136**: 1529–1538.

Narusaka, Y., Nakashima, K., Shinwari, Z.K., Sakuma, Y., Furihata, T., Abe, H., Narusaka, M., Shinozaki, K., and Yamaguchi-Shinozaki, K. (2003). Interaction Between Two cis-Acting Elements, ABRE and DRE, in ABA-Dependent Expression of Arabidopsis rd29A Gene in Response to Dehydration and High-Salinity Stresses. Plant J. **34**: 137–148.

Nomoto, Y., Kubozono, S., Yamashino, T., Nakamichi, N., and Mizuno, T. (2012). Circadian Clock-and PIF4-Controlled Plant Growth: A Coincidence Mechanism Directly Integrates a Hormone Signaling Network into the Photoperiodic Control of Plant Architectures in Arabidopsis thaliana. Plant Cell Physiol. **53**: 1950–1964.

Novillo, F., Alonso, J.M., Ecker, J.R., and Salinas, J. (2004). CBF2/DREB1C is a Negative Regulator of CBF1/DREB1B and CBF3/DREB1A Expression and Plays a Central Role in Stress Tolerance in Arabidopsis. Proc. Natl. Acad. Sci. U. S. A. **101**: 3985–90.

O'Malley, R.C., Barragan, C.C., and Ecker, J.R. (2015). A User's Guide to the Arabidopsis T-DNA Insertion Mutant Collections. Methods Mol. Biol. **1284**: 323–342.

Ohta, M., Guo, Y., Halfter, U., and Zhu, J.-K. (2003). A Novel Domain in the Protein Kinase SOS2 Mediates Interaction with the PROTEIN PHOSPHATASE 2C ABI2. Proc. Natl. Acad. Sci. **100**: 11771–11776.

Okushima, Y., Mitina, I., Quach, H.L., and Theologis, A. (2005). AUXIN RESPONSE FACTOR 2 (ARF2): A Pleiotropic Developmental Regulator. Plant J. **43**: 29–46.

Pahari, S., Cormark, R.D., Blackshaw, M.T., Liu, C., Erickson, J.L., and Schultz, E.A. (2014). *Arabidopsis UNHINGED* encodes a VPS51 Homolog And Reveals A Role for the GARP Complex in Leaf Shape and Vein Patterning. Development **141**: 1894–1905.

Palaniswamy, S.K., James, S., Sun, H., Lamb, R.S., Davuluri, R. V., and Grotewold, E. (2006). AGRIS and AtRegNet. A Platform to Link cis-Regulatory Elements and Transcription Factors into Regulatory Networks. Plant Physiol. **140**: 818–829.

Peng, J., Li, Z., Wen, X., Li, W., Shi, H., Yang, L., Zhu, H., and Guo, H. (2014). Salt-Induced Stabilization of EIN3/EIL1 Confers Salinity Tolerance by Deterring ROS Accumulation in Arabidopsis. PLoS Genet. **10**: e1004664.

Péret, B. et al. (2013). Sequential Induction of Auxin Efflux and Influx Carriers Regulates Lateral Root Emergence. Mol. Syst. Biol. **9**: 699.

Perrot-Rechenmann, C. (2010). Cellular Responses to Auxin: Division Versus Expansion. Cold Spring Harb. Perspect. Biol. **2**: 1–16.

Petersson, S. V., Johansson, A.I., Kowalczyk, M., Makoveychuk, A., Wang, J.Y., Moritz, T., Grebe, M., Benfey, P.N., Sandberg, G., and Ljung, K. (2009). An Auxin Gradient and Maximum in the Arabidopsis Root Apex Shown by High-Resolution Cell-Specific Analysis of IAA Distribution and Synthesis. Plant Cell Online **21**: 1659–1668.

Petricka, J., Winter, C.M., and Benfey, P.N. (2012). Control of Arabidopsis Root

Development. Annnual Rev. Plant Biol. **63**: 563–590.

Prabhakaran-Mariyamma, N. (2015). Elucidating The Role Of The Duf 828 Gene Family Of Arabidopsis Thaliana In Auxin Transport.

Prabhakaran Mariyamma, N., Clarke, K.J., Yu, H., Wilton, E.E., Van Dyk, J., Hou, H., and Schultz, E.A. (2018). Members of the Arabidopsis FORKED1-LIKE Gene Family Act to Localize PIN1 in Developing Veins (Lethbridge).

Prabhakaran Mariyamma, N., Hou, H., Carland, F.M., Nelson, T., and Schultz, E.A. (2017). Localization of Arabidopsis FORKED1 to a RABA-Positive Compartment Suggests a Role in Secretion. J. Exp. Bot. **68**: 3375–3390.

Procko, C., Crenshaw, C.M., Ljung, K., Noel, J.P., and Chory, J. (2014). Cotyledon-Generated Auxin Is Required for Shade-Induced Hypocotyl Growth in Brassica rapa. Plant Physiol. **165**: 1285–1301.

Promchuea, S., Zhu, Y., Chen, Z., Zhang, J., and Gong, Z. (2017). ARF2 Coordinates with PLETHORAs and PINs to Orchestrate ABA-Mediated Root Meristem Activity in Arabidopsis. J. Integr. Plant Biol. **59**: 30–43.

Qi, J., Wang, Y., Yu, T., Cunha, A., Wu, B., Vernoux, T., Meyerowitz, E., and Jiao, Y. (2014). Auxin Depletion from Leaf Primordia Contributes to Organ Patterning. Proc. Natl. Acad. Sci. **111**: 18769–18774.

Quan, R., Wang, J., Yang, D., Zhang, H., Zhang, Z., and Huang, R. (2017). EIN3 and SOS2 Synergistically Modulate Plant Salt Tolerance. Sci. Rep. **7**: 1–11.

Rademacher, E.H., Möller, B., Lokerse, A.S., Llavata-Peris, C.I., Van Den Berg, W., and Weijers, D. (2011). A Cellular Expression Map of the Arabidopsis AUXIN RESPONSE FACTOR Gene Family. Plant J. **68**: 597–606.

Rahman, A., Takahashi, M., Shibasaki, K., Wu, S., Inaba, T., Tsurumi, S., and Baskin, T.I. (2010). Gravitropism of Arabidopsis thaliana Roots Requires the Polarization of PIN2 toward the Root Tip in Meristematic Cortical Cells. Plant Cell **22**: 1762–1776.

Reinhardt, D., Frenz, M., Mandel, T., and Kuhlemeier, C. (2004). Microsurgical and Laser Ablation Analysis of Leaf Positioning and Dorsoventral Patterning in Tomato. Development **132**: 15–26.

Reinhardt, D., Pesce, E.R., Stieger, P., Mandel, T., Baltensperger, K., Bennett, M., Traas, J., Friml, J., and Kuhlemeier, C. (2003). Regulation of Phyllotaxis by Polar Auxin Transport. Nature **426**: 255–260.

Richter, S., Kientz, M., Brumm, S., Nielsen, M.E., Park, M., Gavidia, R., Krause, C., Voss, U., Beckmann, H., Mayer, U., Stierhof, Y.D., and Jürgens, G. (2014). Delivery of Endocytosed Proteins to the Cell-Division Plane Requires Change of Pathway from Recycling to Secretion. Elife **2014**: 1–16.

Rigas, S., Ditengou, F.A., Ljung, K., Daras, G., Tietz, O., Palme, K., and Hatzopoulos, P. (2013). Root Gravitropism and Root Hair Development Constitute Coupled Developmental Responses Regulated by Auxin Homeostasis in the Arabidopsis Root Apex. New Phytol. **197**: 1130–1141.

Robert, H.S. and Friml, J. (2009). Auxin and Other Signals on the Move in Plants. Nat. Chem. Biol. **5**: 325–332.

Rose, A.B., Carter, A., Korf, I., and Kojima, N. (2016). Intron Sequences that Stimulate Gene Expression in Arabidopsis. Plant Mol. Biol. **92**: 337–346.

Rowe, J.H., Topping, J.F., Liu, J., and Lindsey, K. (2016). Abscisic Acid Regulates Root Growth under Osmotic Stress Conditions Via an Interacting Hormonal Network with Cytokinin, Ethylene and Auxin. New Phytol. **211**: 225–239.

Ruegger, M., Dewey, E., Gray, W.M., Hobbie, L., Turner, J., and Estelle, M. (1998). The *TIR1* Protein of Arabidopsis Functions in Auxin Response and is Related to Human *SKP2* and Yeast *Grr1p*. Genes Dev. **12**: 198–207.

Ruzicka, K., Ljung, K., Vanneste, S., Podhorska, R., Beeckman, T., Friml, J., and Benkova, E. (2007). Ethylene Regulates Root Growth through Effects on Auxin Biosynthesis and Transport-Dependent Auxin Distribution. Plant Cell Online **19**: 2197–2212.

Sack, L. and Scoffoni, C. (2013). Tansley Review Leaf Venation : Structure, Function, Development, Evolution, Ecology and Applications in the Past, Present, and Future. New Phytol. **198**: 983–1000.

Sakuma, Y., Liu, Q., Dubouzet, J.G., Abe, H., Shinozaki, K., and Yamaguchi-Shinozaki, K. (2002). DNA-Binding Specificity of the ERF/AP2 Domain of Arabidopsis DREBs, Transcription Factors Involved in Dehydration- and Cold-Inducible Gene Expression. Biochem. Biophys. Res. Commun. **290**: 998–1009.

Sanz, L. et al. (2011). The *Arabidopsis* D-Type Cyclin CYCD2;1 and the Inhibitor ICK2/KRP2 Modulate Auxin-Induced Lateral Root Formation. Plant Cell **23**: 641–660.

Sarojam, R., Sappl, P.G., Goldshmidt, A., Efroni, I., Floyd, S.K., Eshed, Y., and Bowman, J.L. (2010). Differentiating Arabidopsis Shoots from Leaves by Combined YABBY Activities. Plant Cell Online **22**: 2113–2130.

Sauer, M., Balla, J., Luschnig, C., Wis, J., and Reinöhl, V. (2006). Regulation of PIN Polarity Canalization of Auxin Flow by Aux / IAA-ARF-Dependent Feedback Regulation of PIN Polarity. Genes Dev. **20**: 2902–2911.

Scarpella, E., Marcos, D., Friml, J., Berleth, T., Scarpella, E., Marcos, D., and Berleth, T. (2006). Control of Leaf Vascular Patterning by Polar Auxin Transport Control of Leaf Vascular Patterning by Polar Auxin Transport. **20**: 1015–1027.

Scheres, B., Wolkenfelt, H., Willemsen, V., Terlouw, M., Lawson, E., Dean, C., and Weisbeek, P. (1994). Embryonic Origin of the Arabidopsis Primary Root and Root Meristem Initials. Development **120**: 2475–2487.

Scoffoni, C., Vuong, C., Diep, S., Cochard, H., and Sack, L. (2013). Leaf Shrinkage with Dehydration: Coordination with Hydraulic Vulnerability and Drought Tolerance.

Seo, P.J. and Park, C. (2009). Auxin Homoeostasis During Lateral Root Development under Drought Condition. Plant Signal. Behav. **4**: 1002–1004.

Shen, Q.J., Casaretto, J.A., Zhang, P., and Ho, T.H.D. (2004). Functional Definition of ABA-Response Complexes: The Promoter Units Necessary and Sufficient for ABA Induction of Gene Expression in Barley (Hordeum vulgare L.). Plant Mol. Biol. **54**: 111–124.

Shinozaki, K. and Yamaguchi-Shinozaki, K. (2000). Molecular Responses to Dehydration and Low Temperature: Differences and Cross-Talk Between Two Stress Signaling Pathways. Curr. Opin. Plant Biol. **3**: 217–223.

Sieburth, L.E., Muday, G.K., King, E.J., Benton, G., Kim, S., Metcalf, K.E., Meyers, L., Seamen, E., and Van Norman, J.M. (2006). SCARFACE Encodes an ARF-GAP that is Required for Normal Auxin Efflux and Vein Patterning in Arabidopsis. Plant Cell **18**: 1396–1411.

Simonini, S., Deb, J., Moubayidin, L., Stephenson, P., Valluru, M., Freire-Rios, A., Sorefan, K., Weijers, D., Friml, J., and Østergaard, L. (2016). A Noncanonical Auxin-Sensing Mechanism is Required for Organ Morphogenesis in Arabidopsis. Genes Dev. **30**: 2286–2296.

Singh, M., Gupta, A., and Laxmi, A. (2017). Striking the Right Chord: Signaling Enigma during Root Gravitropism. Front. Plant Sci. **8**: 1–17.

Stepanova, A.N., Robertson-Hoyt, J., Yun, J., Benavente, L.M., Xie, D.Y., Doležal, K., Schlereth, A., Jürgens, G., and Alonso, J.M. (2008). TAA1-Mediated Auxin Biosynthesis Is Essential for Hormone Crosstalk and Plant Development. Cell **133**: 177–191.

Steynen, Q.J. and Schultz, E.A. (2003). The FORKED Genes are Essential for Distal Vein Meeting in Arabidopsis. Development **130**: 4695–4708.

Su, Z., Ma, X., Guo, H., Sukiran, N.L., Guo, B., Assmann, S.M., and Ma, H. (2013). Flower Development under Drought Stress: Morphological and Transcriptomic Analyses Reveal Acute Responses and Long-Term Acclimation in Arabidopsis. Plant Cell **25**: 3785–3807.

Sukumar, P., Edwards, K.S., Rahman, A., DeLong, A., and Muday, G.K. (2009). PINOID Kinase Regulates Root Gravitropism through Modulation of PIN2-Dependent Basipetal Auxin Transport in Arabidopsis. Plant Physiol. **150**: 722–735.

Swarup, K. et al. (2008). The auxin influx carrier LAX3 promotes lateral root emergence. Nat. Cell Biol. **10**: 946–954.

Swarup, R., Perry, P., Hagenbeek, D., Van Der Straeten, D., Beemster, G.T.S., Sandberg, G., Bhalerao, R., Ljung, K., and Bennett, M.J. (2007). Ethylene Upregulates Auxin Biosynthesis in Arabidopsis Seedlings to Enhance Inhibition of Root Cell Elongation. Plant Cell Online **19**: 2186–2196.

Tao, Y. et al. (2008). Rapid Synthesis of Auxin Via a New Tryptophan-Dependent Pathway is Required for Shade Avoidance in Plants. Cell **133**: 164–176.

Thole, J.M., Beisner, E.R., Liu, J., Venkova, S. V., and Strader, L.C. (2014). Abscisic Acid Regulates Root Elongation Through the Activities of Auxin and Ethylene in Arabidopsis thaliana. G3 Genes, Genomes, Genet. **4**: 1259–1274.

Trupkin, S.A., Auge, G.A., Zhu, J.-K., Sánchez, R.A., and Botto, J.F. (2017). SALT OVERLY SENSITIVE 2 (SOS2) and Interacting Partners SOS3 and ABSCISIC ACID–INSENSITIVE 2 (ABI2) Promote Red-Light-Dependent Germination and Seedling Deetiolation in *Arabidopsis*. Int. J. Plant Sci. **178**: 485–493.

Ulmasov, T., Hagen, G., and Guilfoyle, T.J. (1999). Dimerization and DNA binding of auxin response factors. Plant J. **19**: 309–319.

Untergasser, A. (2008). Preparation of Electro-Competent Cells. Untergasser's Lab.

Vanderauwera, S., Vandenbroucke, K., Inze, A., van de Cotte, B., Muhlenbock, P., De Rycke, R., Naouar, N., Van Gaever, T., Van Montagu, M.C.E., and Van Breusegem, F. (2012). AtWRKY15 Perturbation Abolishes the Mitochondrial Stress Response that Steers

Osmotic Stress Tolerance in Arabidopsis. Proc. Natl. Acad. Sci. **109**: 20113–20118.

Vanneste, S., Maes, L., De Smet, I., Himanen, K., Naudts, M., Inzé, D., and Beeckman, T. (2005). Auxin Regulation of Cell Cycle and its Role During Lateral Root Initiation. Physiol. Plant. **123**: 139–146.

Vernoux, T., Besnard, F., and Traas, J. (2010). Auxin at the Shoot Apical Meristem. Cold Spring Harb Perspect Biol. **2**: a001487.

Viczián, A., Kircher, S., Fejes, E., Millar, A.J., Schäfer, E., Kozma-Bognár, L., and Nagy, F. (2005). Functional Characterization of Phytochrome Interacting Factor 3 for the Arabidopsis Thaliana Circadian Clockwork. Plant Cell Physiol. **46**: 1591–1602.

Vishwakarma, K., Upadhyay, N., Kumar, N., Yadav, G., Singh, J., Mishra, R.K., Kumar, V., Verma, R., Upadhyay, R.G., Pandey, M., and Sharma, S. (2017). Abscisic Acid Signaling and Abiotic Stress Tolerance in Plants: A Review on Current Knowledge and Future Prospects. Front. Plant Sci. **08**: 1–12.

Waadt, R., Hitomi, K., Nishimura, N., Hitomi, C., Adams, S.R., Getzoff, E.D., and Schroeder, J.I. (2014). FRET-Based Reporters for the Direct Visualization of Abscisic Acid Concentration Changes and Distribution in Arabidopsis. Elife **3**: e01739.

Wang, L., Hua, D., He, J., Duan, Y., Chen, Z., Hong, X., and Gong, Z. (2011a). Auxin Response Factor2 (ARF2) and its Regulated Homeodomain Gene HB33 Mediate Abscisic Acid Response in Arabidopsis. PLoS Genet. **7**: e1002172.

Wang, W., Xu, B., Wang, H., Li, J., Huang, H., and Xu, L. (2011b). YUCCA Genes Are Expressed in Response to Leaf Adaxial-Abaxial Juxtaposition and Are Required for Leaf Margin Development. Plant Physiol. **157**: 1805–1819.

Wenzel, C.L., Schuetz, M., Yu, Q., and Mattsson, J. (2007). Dynamics of MONOPTEROS and PIN-FORMED1 Expression During Leaf Vein Pattern Formation in Arabidopsis thaliana. Plant J. **49**: 387–398.

de Wit, M., Ljung, K., and Fankhauser, C. (2015). Contrasting Growth Responses in Lamina and Petiole During Neighbor Detection Depend on Differential Auxin Responsiveness Rather than Different Auxin Levels. New Phytol. **208**: 198–209.

Won, C., Shen, X., Mashiguchi, K., Zheng, Z., Dai, X., Cheng, Y., Kasahara, H., Kamiya, Y., Chory, J., and Zhao, Y. (2011). Conversion of Tryptophan to Indole-3-Acetic Acid by TRYPTOPHAN AMINOTRANSFERASES OF ARABIDOPSIS and YUCCAs in Arabidopsis. Proc. Natl. Acad. Sci. **108**: 18518–18523.

Woodward, A.W. and Bartel, B. (2005). Auxin: Regulation, Action, and Interaction. Ann. Bot. **95**: 707–735.

Xia, Y., Chu, W., Qi, Q., and Xun, L. (2015). New Insights into the QuikChangeTM Process Guide the use of Phusion DNA Polymerase for Site-Directed Mutagenesis. Nucleic Acids Res. **43**: e12.

Xie, Y., Liu, Y., Wang, H., Ma, X., Wang, B., Wu, G., and Wang, H. (2017). Phytochrome-Interacting Factors Directly Suppress MIR156 Expression to Enhance Shade-Avoidance Syndrome in Arabidopsis. Nat. Commun. **8**: 1–11.

Yamaguchi, T., Nukazuka, A., and Tsukaya, H. (2012). Leaf Adaxial-Abaxial Polarity Specification and Lamina Outgrowth: Evolution and Development. Plant Cell Physiol. **53**:

1180–1194.

Yilmaz, A., Mejia-Guerra, M.K., Kurz, K., Liang, X., Welch, L., and Grotewold, E. (2011). AGRIS: The Arabidopsis Gene Regulatory Information Server, an Update. Nucleic Acids Res. **39**: 1118–1122.

Yoshida, T., Fujita, Y., Maruyama, K., Mogami, J., Todaka, D., Shinozaki, K., and Yamaguchi-Shinozaki, K. (2015). Four Arabidopsis AREB/ABF Transcription Factors Function Predominantly in Gene Expression Downstream of SnRK2 Kinases in Abscisic Acid Signalling in Response to Osmotic Stress. Plant, Cell Environ. **38**: 35–49.

Yuan, F. et al. (2014). OSCA1 Mediates Osmotic-Stress-Evoked Ca2+Increases Vital for Osmosensing in Arabidopsis. Nature **514**: 367–371.

de Zelicourt, A., Colcombet, J., and Hirt, H. (2016). The Role of MAPK Modules and ABA during Abiotic Stress Signaling. Trends Plant Sci. **21**: 677–685.

Zhang, J., Jia, W., Yang, J., and Ismail, A.M. (2006). Role of ABA in Integrating Plant Responses to Drought and Salt Stresses. F. Crop. Res. **97**: 111–119.

Zhang, J., Nodzynski, T., Pencik, A., Rolcik, J., and Friml, J. (2010). PIN Phosphorylation is Sufficient to Mediate PIN Polarity and Direct Auxin Transport. Proc. Natl. Acad. Sci. **107**: 918–922.

Zhao, Y. et al. (2016). ABA Receptor PYL9 Promotes Drought Resistance and Leaf Senescence. Proc. Natl. Acad. Sci. **113**: 1949–1954.

Zhao, Y. (2012). Auxin Biosynthesis: A Simple Two-Step Pathway Converts Tryptophan to Indole-3-Acetic Acid in plants. Mol. Plant **5**: 334–338.

Zhao, Y. (2010). Auxin Biosynthesis and its role in plant development. Annu. Rev. Plant Biol. **40**: 49–64.

Zhao, Y., Wang, T., Zhang, W., and Li, X. (2011). SOS3 Mediates Lateral Root Development Under Low Salt Stress Through Regulation of Auxin Redistribution and Maxima in Arabidopsis. New Phytol. **189**: 1122–1134.

Zhu, J.-K. (2016). Abiotic Stress Signaling and Responses in Plants. Cell **167**: 313–324.

Zolla, G., Heimer, Y.M., and Barak, S. (2010). Mild Salinity Stimulates a Stress-Induced Morphogenic Response in Arabidopsis thaliana Roots. J. Exp. Bot. **61**: 211–224.

Zwieniecki, M.A. and Boyce, C.K. (2014). Evolution of a Unique Anatomical Precision in Angiosperm Leaf Venation Lifts Constraints on Vascular Plant Ecology. Proc. R. Soc. B Biol. Sci. **281**: 20132829.